REPORT NO.
UCB/EERC-87/03
APRIL 1987

EARTHQUAKE ENGINEERING RESEARCH CENTER

A DISPLACEMENT CONTROL AND UPLIFT RESTRAINT DEVICE FOR BASE ISOLATED STRUCTURES

by

JAMES M. KELLY
MICHAEL C. GRIFFITH
IAN D. AIKEN

Report to the National Science Foundation

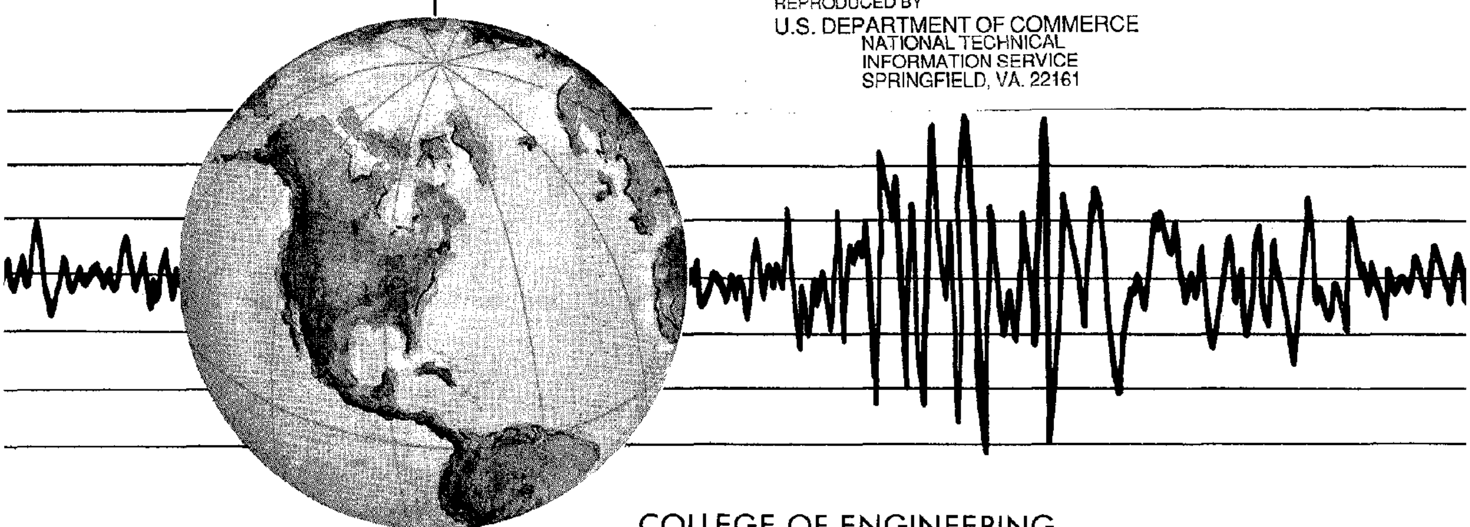

COLLEGE OF ENGINEERING

UNIVERSITY OF CALIFORNIA • Berkeley, California

For sale by the National Technical Information Service, U.S. Department of Commerce, Springfield, Virginia 22161.

See back of report for up to date listing of EERC reports.

DISCLAIMER

50272-101

REPORT DOCUMENTATION PAGE	1. REPORT NO. NSF/ENG-87031 1a	2.	3. Recipient's Accession No. PB88-169933

4. Title and Subtitle A Displacement Control and Uplift Restraint Device for Base Isolated Structures	**5. Report Date** April 1987
	6.
7. Author(s) James M. Kelly, Michael C. Griffith and Ian D. Aiken	**8. Performing Organization Rept. No.** UCB/EERC-87/03
9. Performing Organization Name and Address Earthquake Engineering Research Center, University of California, Berkeley, 1301 South 46th Street, Richmond, Ca. 94804	**10. Project/Task/Work Unit No.**
	11. Contract(C) or Grant(G) No. (C) (G) ECE-8414036
12. Sponsoring Organization Name and Address National Science Foundation, 1800 G. Street, N.W., Washington, D.C. 20550	**13. Type of Report & Period Covered**
	14.

15. Supplementary Notes

16. Abstract (Limit: 200 words)

A displacement control device that can be installed within multilayer elastomeric base isolation bearings is described. The device acts to limit the displacement of the bearings and can also be used to take uplift tension forces if necessary.

The device was tested in earthquake simulator tests of a nine-story, 1/4-scale steel frame model, at the Earthquake Simulator Laboratory of the Earthquake Engineering Research Center, University of California at Berkeley. The model was isolated using eight multilayer elastomeric bearings, four of which were located at the corners of the model and contained the displacement control devices.

The system was subjected to a large number of simulated earthquakes. In some tests the design acted to control the displacements and in others where uplift forces at the corners were generated the devices simultaneously limited the displacements and carried the uplift forces.

The test results show that the action of the devices is smooth and that there is no sudden jerk when one comes into action. The devices can perform as a fail-safe system for base isolated buildings: in this role they would be designed to act only when the ground motion is greater than that for which the base isolation system has been designed.

17. Document Analysis a. Descriptors

earthquake
base isolated
uplift
elastomeric

b. Identifiers/Open-Ended Terms

displacement control
base isolation
elastomeric bearings
uplift forces

c. COSATI Field/Group

18. Availability Statement	**19. Security Class (This Report)**	**21. No. of Pages**
Release unlimited	Unclassified	72
	20. Security Class (This Page) Unclassified	**22. Price** A04 14.95

(See ANSI-Z39.18) See Instructions on Reverse OPTIONAL FORM 272 (4-77) (Formerly NTIS-35) Department of Commerce

ib

A DISPLACEMENT CONTROL AND UPLIFT RESTRAINT DEVICE FOR BASE ISOLATED STRUCTURES

by

James M. Kelly

Michael C. Griffith

Ian D. Aiken

A report on research sponsored by

the National Science Foundation

(Grant ECE-8414036)

Report No. UCB/EERC-87/03

Earthquake Engineering Research Center

University of California

Berkeley, California

April 1987

ABSTRACT

A displacement control device that can be installed within multilayer elastomeric base isolation bearings is described. The device acts to limit the displacement of the bearings and can also be used to take uplift tension forces if necessary.

The device was tested in earthquake simulator tests of a nine-story, 1/4-scale steel frame model, conducted at the Earthquake Simulator Laboratory of the Earthquake Engineering Research Center, University of California, Berkeley. The model was isolated using eight multilayer elastomeric bearings, four of which were located at the corners of the model and contained the displacement control devices.

The system was subjected to a large number of simulated earthquakes. In some tests the design acted to control the displacements and in others where uplift forces at the corners were generated the devices simultaneously limited the displacements and carried the uplift forces.

The test results show that the action of the devices is smooth and that there is no sudden jerk when one comes into action. The devices can perform as a fail-safe system for base isolated buildings: in this role they would be designed to act only when the ground motion is greater than that for which the base isolation system has been designed.

ACKNOWLEDGMENTS

The research reported herein was supported by the National Science Foundation under Grant No. ECE-8414036, and was conducted at the Earthquake Engineering Research Center of the University of California at Berkeley. Views expressed herein are those of the authors and not necessarily those of the sponsor.

The staff of the Earthquake Engineering Research Center, especially Messrs. D. Clyde, I. Van Asten, Drs. J. S. Dimsdale, C. M. Uang and Beverley Bolt provided invaluable assistance and advice over the course of the experimentation.

TABLE OF CONTENTS

LIST OF TABLES

LIST OF FIGURES

1. INTRODUCTION

Base isolation is becoming a widely accepted seismic design strategy for low-rise, stiff buildings in highly seismic regions. It has been used and has been proposed for new buildings of up to five stories and as a seismic rehabilitation technique for existing buildings of up to seven stories. It is especially well suited to stiff structures since the degree of attenuation produced by the isolation system depends on the difference between the period of the building when isolated and its period as a fixed base structure. If the isolation period is 2.0 seconds and the fixed base period is 0.5 second a reduction in base shear force of 75% to 80% is possible. An isolation period of around 3 seconds is the longest period that can be achieved by practical systems that utilize elastomeric isolation bearings; and thus it has generally been accepted that isolation may not be possible for medium-rise buildings, since the necessary spread of period between the fixed-base structure and the isolated structure cannot not be achieved. Nevertheless, many medium-rise buildings can be quite stiff and isolation could still be effective in reducing the seismic base shear.

It has generally been accepted that elastomeric isolators should not be expected to take tension. A medium-rise building (10-15 stories), even when isolated, could generate an overturning moment that would cause uplift on some isolators. If a method could be devised to enable the elastomeric isolators to sustain tension then the technique could be extended to a building with a larger number of stories than has so far been contemplated, provided that the superstructure of the building is sufficiently stiff to have a fixed base period not longer than 1 second. The tension that would have to be sustained by the isolators would, of course, be transmitted to the foundation but this tension would be an order of magnitude less than that which would have to be carried by the foundation if the building were conventionally designed, since the overturning moment for the isolated building would be significantly less than that for the comparable conventional building. In a conventional design the overturning moment is concentrated at the core and the foundation elements under the core need to sustain high tension forces. In an isolated building the tension is widely distributed over bearings which cover the entire plan area.

Some tension capacity in the isolation bearings would be advantageous for both low-rise and medium-rise buildings for another reason. The base isolation approach, although a very old concept, is still relatively recent in implementation and there is still resistance among engineers to its use. While it is recognized that designing a structure by code will produce a building able to withstand a moderate earthquake with little damage, it is believed that such a code designed building will survive a very large earthquake, e.g. Richter magnitude 8, with damage and possibly very severe damage, but will not collapse. The presence of member ductility and design redundancy will enable the structure to survive. In a base isolated structure, on the other hand, this ductility and redundancy do not appear to be present. It is easy to design an isolation system for a code specified design earthquake, but the performance of the isolation system if the earthquake is very much larger than the design earthquake is not clear. The isolation system seems to be the only line of defense and if this fails collapse seems to be inevitable. This shortcoming is continually raised and has led to the abandonment of promising designs using base isolation. For these reasons, a fail-safe system which would come into play when the earthquake intensity at the site exceeds that for which the building was designed is needed to eliminate this uncertainty.

Fail-safe systems to be used with isolation systems have of course been designed. In some, the building comes against a stop when the design displacement or some factor times the design displacement is exceeded [1]. Another approach is to have sliding surfaces, separated by a small clearance, which come into contact beyond a specified horizontal displacement so that the vertical load is transferred from the bearings to the sliding surfaces reducing the chance of collapse and increasing damping through friction [2]. Both of these have obvious disadvantages among which is cost. What is needed is a simple low-cost modification to the isolation system that would control the displacements if the earthquake intensity became too great.

In this report we will describe such a system and show that it is effective and practical. The system fits within a standard elastomeric bearing requiring no modification of the foundation or surrounding retaining wall. Its effectiveness has been demonstrated by tests on the earthquake simulator at the Earthquake Engineering Research Center (EERC) of the University of California at Berkeley. It has been used in an isolation system tested under a tall steel-frame model which, under moderate earthquake loading, generated uplift forces on the bearings.

The tests demonstrated that the displacement control device plays the role of a fail-safe system for low-rise buildings by smoothly limiting the maximum displacement under any level of earthquake. It will also act as a tension restraining device for tall base-isolated structures by taking the uplift forces generated by any earthquake loading that would produce uplift in unmodified bearings.

It is felt that this device will allow the profession to proceed with the design of base-isolated structures with confidence that a low-cost effective structural system will not collapse if the design earthquake is exceeded. Thus, since the base-isolated structure will be able to survive moderate earthquakes with no damage and with elastic response, the structural design for seismic loading will be greatly simplified and a better performing structure will result.

2. PROPERTIES OF THE TEST STRUCTURE

The shaking table experiments were carried out on a nine-story three-bay welded steel frame model (Figure 2.1). The lowest story of the model was 4 feet high and the others were 3 feet high. The top of the model was almost 29 feet above the top of the isolation bearings and the width of the model was 18 feet. The aspect ratio was large enough that the model would experience uplift in the corner columns with moderate accelerations in the structure.

The model was not specifically designed for this test series but was adapted from that of a previous series of uplift tests [3]. The model represents a section in the weak direction of a typical steel-frame building at approximately 1/4-scale. The additional mass necessary for similitude requirements was provided by concrete blocks at each floor level. The total weight of the structure and the concrete blocks was 122 kips. The two rows of columns were bolted to stiff wide flange sections (W8x31) which ran the length of the base of the model, and with cross beams these represented the base mat of a prototype structure. The base isolators were placed between these W8x31 beams and the shaking table.

The test structure was instrumented with accelerometers, linear potentiometers, and direct current displacement transducers to enable accurate time history records of the responses of the model to be recorded for subsequent analysis. Each bearing was supported by a force transducer [4], from which time series records of the forces acting on the bearing were collected (Figure 2.2). The shear force at the base of the model structure was calculated for all excitations using the data acquired from these force transducers, and then compared with the base shear obtained by summing the inertial story shears. The correlation of these values was within about 10%.

The first two natural frequencies of the fixed base model structure (attached rigidly to the shaking table) were 2.8 Hz and 9.0 Hz. These were determined by taking fast Fourier transforms (FFTs) of the ninth floor horizontal acceleration time history when the model was subjected to a free-vibration pull-back test. In a similar fashion the first three natural frequencies of the base-isolated model were found to be 1.11 Hz, 6.09 Hz, and 13 Hz.

The 0.901 second period of the base-isolated 1/4-scale structure corresponds to a 1.8 second period for the prototype structure. This is a realistic value for a base-isolated structure, the practical upper limit being about 2 to 3 seconds. Although the period shift was not as great as is usually desired (an increase of 3 to 4 times is common), it was shown that the isolation with this shift in period still provided significant reductions in base shear and story accelerations from the fixed base design values.

3. ISOLATION SYSTEM

The isolation system consisted of eight natural rubber bearings of multilaminate construction with a bearing located under each column of the steel frame. The natural rubber compound used in these bearings is designated EDS 39 [5] by the Malaysian Rubber Producers Research Association (MRPRA). It is a high strength lightly filled rubber which has a shear modulus of approximately 100 psi at 50% shear strain. It is relatively low in damping; the equivalent viscous damping ratio at 50% shear strain is in the range of 5% to 7%.

The bearings (Figure 3.1) are 6 inches square in plan and have six layers of 3/8-inch thick rubber, 5 reinforcing shims of 1/8-inch thickness and 1 inch thick top and bottom end plates. They also have central holes of 1.25 inches diameter. The bearings are designed with four dowel holes top and bottom to provide shear connections between the isolation system and the structure. When the uplift restrainers were not in place the dowel holes contained 3/4-inch long pins. In this configuration the frame was free to uplift and no tension was generated in the rubber.

Each bearing provided a stiffness of 1.6 kips/inch at 50% shear strain (or 1.125 inches displacement) which provided an isolation frequency for the model of 1.01 Hz. This frequency was too low to generate uplift forces at the corner columns for this model since the isolation system did not permit enough transmission of acceleration to the model to generate tension in the corner columns. In order to increase the likelihood of uplift, lead plugs were inserted in the central holes of the four bearings under the center columns. Lead yields at a stress of approximately 1500 ksi which corresponded to 1.8 kips shear load in a lead plug, and at 50% shear strain the effective contribution of each lead plug to the stiffness was 1.6 kips/inch. With the four bearings filled with lead the isolation frequency at 50% shear strain rose to 1.24 Hz. The increased stiffness and the tendency of the lead plugs to generate response in the higher modes made uplift more probable with moderate table inputs.

A device that provides uplift restraint and displacement control was inserted in each of the four corner bearings (Figure 3.2). This displacement control device is shown in Figure 3.3. It consists of two high-strength bolts contained in a cylindrical sleeve that allows a certain amount of free movement of the bolts. The devices have hemispherical ends held in hemispherical recesses which were machined into the 1 inch thick top and bottom plates of the bearings. When the bearing is not displaced the bolt heads are together in the center of the sleeve and when the bearing is displaced through a preselected distance the device becomes taut. Since uplift occurs at maximum displacements the device will also resist the uplift forces in addition to acting as a displacement control device. A further modification necessary to enable the bearing to resist uplift is that the four dowel holes in each end plate be threaded and the bearing firmly connected to the foundation (in this case the load cell under the bearing) and to the superstructure. If displacement control only is needed it is unnecessary to bolt the bearings to the foundation and the superstructure and dowels can be retained to transfer shear loads. It should be noted that the lead plugs in the center four bearings were used in these tests only for the purpose of producing uplift at the corners at moderate levels of earthquake input. They are not an essential component of the isolation system.

4. DEVICE FOR UPLIFT RESTRAINT AND DISPLACEMENT CONTROL

The device used in the test series to provide both uplift restraint and displacement control, described in the previous chapter, used two bolts within a cylindrical sleeve. The bolts can move a certain distance (which can be adjusted) within the cylindrical sleeve, but when the bearing has displaced horizontally through this distance the bolt heads are constrained by the ends of the sleeve. At this displacement the horizontal stiffness of the bearing is greatly increased. While this results in a sudden increase in stiffness there is not a sudden stop because, although the restraint device is now inextensible, the bearing can continue to deform horizontally by deforming vertically at the same time. Thus, the horizontal stiffness which is normally low becomes comparable with the much higher vertical stiffness.

Tests were performed on individual bearings in a testing device (Figure 4.1) which applied a constant axial load to the bearings while forcing them through several cycles of constant amplitude sinusoidal displacement. Force versus displacement curves were obtained from these tests at several different displacement amplitudes (Figure 4.2). Possibly because of friction between the device and the surface of the hole in the bearing, the transition from the stiffness at low shear strain to the combined stiffness of the bearing and the restrainer device at high shear strains was smooth. This smooth transition in stiffness at the initial operating displacement (u_d) of the device had the effect of minimal excitation of higher structural frequencies and led to a far better structural response than might have been expected if the stiffness had been sharply bilinear.

A linear elastic analysis of the response of the bearing with the device was carried out taking into account the vertical and horizontal stiffnesses of the natural rubber bearing, the displaced geometry of the bearing, and assuming small strains in the steel restrainer (Figure 4.3) and a constant axial dead load (W) on the bearing. With these assumptions the following relationship for force versus displacement of the uplift restrainer bearing was obtained. The derivation is given in Appendix A.

$$F_x = k_h u_x \qquad \text{for } u_x \leq u_d \tag{4.1}$$

and

$$F_x = k_h u_d + \left[k_h + \frac{k_v u_d^2}{h^2 + \frac{k_v}{k_d} L^2} \right] e_x \qquad \text{for } u_x \geq u_d \tag{4.2}$$

with

$$u_d = \left[L^2 - h^2 \right]^{\frac{1}{2}} \tag{4.3}$$

and

$$u_x = u_d + e_x \; ; \tag{4.4}$$

where

F_x = shear force applied to the bearing

W = axial dead load on the bearing

P = axial force in displacement control device

k_h, k_v = horizontal & vertical bearing stiffnesses, respectively

k_d = axial stiffness of restrainer device

u_x = total horizontal bearing displacement

u_d = horizontal bearing displacement when $P = 0^+$

$e_x = u_x - u_d$

u_y = vertical displacement of bearing due to P

δ_y = decrease in bearing height due to W

$h = H$ – thickness of end plates – δ_y

L = length of restrainer when device begins to act

u_L = increase in length of restrainer due to P .

The experimentally obtained force-displacement curves for the restrained bearing and the curve predicted by the equations above are given in Figure 4.4.

5. TEST PROGRAM

The model was subjected to eight different earthquake signals on the shaking table. The earthquake characteristics ranged from predominantly low frequency ground motion (Mexico City and Bucharest) to predominantly high frequency ground motion (San Francisco). The earthquake test signals used were digitized records based on the earthquake ground motion data recorded at the sites listed below [6-9].

(1) Imperial Valley Earthquake (El Centro) of May 18, 1940 — S00E component, peak ground acceleration (PGA) = 0.35g

(2) Kern County Earthquake (Taft Lincoln School Tunnel) of July 21, 1952 — S69E component, PGA = 0.18g

(3) San Francisco Earthquake (Golden Gate Park) of March 22, 1957 — S80E component, PGA = 0.10g

(4) Parkfield Earthquake (Cholame, Shandon, Calif. Array No. 2) of June 27, 1966 — N65E component, PGA = 0.49g

(5) San Fernando Earthquake (Pacoima Dam) of February 9, 1971 — S14W component, PGA = 1.08g

(6) Bucharest Earthquake (Building Research Institute) of March 7, 1977 — EW component, PGA = 0.21g

(7) Miyagi-Ken-Oki Earthquake (Tohoku University) of June 12, 1978 — S00E component, PGA = 0.24g

(8) Mexico City Earthquake (Mexico City Station SCT) of September 19, 1985 — S60E component, PGA = 0.20g

The records were time-scaled (compressed) by a factor of two to satisfy similitude requirements for the 1/4-scale model.

Plots of the real time earthquake ground motions normalized to 1.0g peak acceleration and their FFTs are given in Figures 5.1 and 5.2, respectively. These FFT plots indicate the wide range of earthquake characteristics represented by this group of earthquakes. The time-scaled Mexico City signal has its energy content concentrated almost entirely in the region of 0.5 Hz; the time-scaled Bucharest signal has a significant amount of low frequency energy which gradually decreases to near zero at a frequency of about 5 Hz; El Centro has most of its energy between 1 Hz and 3 Hz; Miyagi has most of its energy around 1 Hz; Parkfield, 0.5 Hz to 3 Hz; Pacoima Dam, 1 Hz to 4 Hz; San Francisco has a peak near 4 Hz and another at about 7 Hz; and Taft has a wide range of frequency (0.5 Hz to 5 Hz) over which there is a significant amount of input energy.

The earthquake signals used in the testing program and the nomenclature used throughout the rest of this report are given in Table 5.1 and a list of the scale factors necessary for converting the experimental results for the 1/4-scale model to values for a prototype structure is given in Table 5.2. Table 5.3 lists the input signals used in the testing program and the maximum model responses to the input signals for the tests on the model in the free-to-uplift condition. Table 5.4 lists the maximum responses of the model when it was restrained against uplift.

6. TEST RESULTS

Each of the earthquake test signals was used to excite the model at various levels of input magnitude. It was thought that uplift could be achieved with moderate levels of input and so the test signals chosen for extensive tests at or near uplift were the Bucharest, Mexico City, and El Centro signals. The dominant frequency content of these time-scaled signals ranged from about 1.0 Hz for the Mexico City signal to about 4 Hz for El Centro.

Maximum model acceleration was plotted against maximum table acceleration for the three signals (Figure 6.1). These plots indicate that the structure acceleration required to cause corner column uplift was about 0.44g. This result depends on the vertical distribution of acceleration in the structure but for the range of frequency associated with the test signals the distribution was essentially uniform. The bearing displacement associated with the 0.44g acceleration required for uplift was about 2.2 inches. This information was used to estimate the amount of free horizontal bearing displacement to allow before the displacement control device should begin to carry any load.

Free-to-Uplift Model

Each earthquake input signal was run at increasing peak table acceleration until the model lifted off the unrestrained corner bearings. Time histories of bearing horizontal displacement and column vertical displacement (Figure 6.2) showed that significant column uplift occurred (0.75 inch) during the El Centro-0.842g test. The results for the 1/4-scale model implied 3 inches of column uplift of the corner columns in the prototype structure. The Mexico City-0.217g test caused 0.47 inch column uplift and the Bucharest-0.348g test caused 0.61 inch column uplift. It should also be noted from Figure 6.2 that the column uplift occurred at the time of peak horizontal displacement.

In view of the large vertical accelerations generated in the structure when the structure dropped back to its foundation, column uplift was undesirable. The vertical accelerations which occurred in the model when the structure was subjected to the El Centro motion (0.75 inch uplift) are shown in Figure 6.3. The peaks in vertical acceleration response could be eliminated by preventing column uplift and then any structural response sensitive to vertical accelerations would be improved.

The effect of uplift on the force-displacement relationships of the bearings is shown in Figure 6.4. Although the bearings dissipated little energy axially during the uplift motion they did continue to dissipate energy in shear. The column uplift distorted the shapes of both the shear and axial hysteresis loops. The effect of column uplift on the axial hysteresis loop is clear — the vertical displacement of the column base increased from about 0.1 inch to about 0.75 inch without any change in the axial load on the bearing. Column axial load appears to have more of an effect on the shear hysteresis loop when it comes back into contact with the bearing than when it lifts off the bearing. Keeping in mind the fact that positive horizontal displacement corresponds to tensile axial load on the bearing, the shear hysteresis loop appears to become unstable at the time of maximum compressive load (15 kips due to overturning plus the bearing dead load of 8 kips). This was probably due to the combination of a decrease in the thickness of the rubber layers and a sudden drop in shear stiffness because of the sudden increase in axial load on the bearing. This phenomenon would probably only be observed in cases where the axial loads approach the buckling load. Nevertheless, this behavior is clearly undesirable since any sudden drop in the stiffness of the isolation system could result in significantly larger bearing displacements.

By studying the acceleration profiles (Figure 6.5) for each earthquake at different values of peak acceleration it is seen that the effectiveness of the isolation system depended greatly on the earthquake frequency content. For an earthquake with the major part of its frequency content concentrated near the resonant frequency of the isolated structure the effectiveness of the isolation system was limited — for example, the Mexico City and Bucharest earthquakes, for which input accelerations were actually amplified in the structure by the isolation system. The San Francisco test signal showed that the isolation system provided significant reductions in structural accelerations for earthquake motions with the dominant portion of their frequency content well removed from the frequency of the isolated structure. The effect of column uplift on the story acceleration profile was demonstrated by the sequence of tests with the Bucharest, Mexico City, and El Centro signals. For the other test signals the acceleration profiles decrease in magnitude with increased table acceleration. This was probably due to the nonlinear stiffness of the bearings. As the bearing displacement increased with table intensity, the effective stiffness decreased. Thus, the frequency of the isolated structure decreased and shifted away from the dominant excitation frequencies for the Miyagi-Ken-Oki, Pacoima Dam, Parkfield, San Francisco, and Taft earthquake signals.

Although significant column uplift occurred during the largest magnitude tests using the three test signals the bearing shear connection did not uncouple as happened during previous tests performed on a base-isolated reinforced concrete structure [10]. Recognizing the importance of preventing uncoupling of the bearings during extreme uplift events, longer dowels were designed for this test series to overcome the problem. A dowel length of 0.75 inch was used, and this proved to be sufficient to prevent uncoupling.

The plots of peak base shear ratio versus maximum table acceleration (Figure 6.6) indicate that the rate of increase in base shear decreases with increasing shaking table acceleration for the El Centro signal. For the Mexico City tests, however, the base shear ratio increased dramatically around 0.18g. This was due to the fact that the decrease in the bearing stiffness helped to bring the isolation frequency into resonance with the Mexico City signal. This was possible since the isolation frequency at small shear strains was higher than the dominant frequency content of the Mexico signal.

This same effect, but to a lesser extent, was also observed during the sequence of Bucharest earthquake tests. The El Centro sequence of tests was nearly linear, except for the largest magnitude test (0.842g peak table acceleration) when significant column uplift occurred. The value of 34.3%W (maximum base shear as a percentage of the total structure weight) for the free-to-uplift model subjected to the El Centro signal with a peak table acceleration of 0.842g contrasts with 20%W for the structure when fixed at its base and subjected to the El Centro input signal having a 0.110g peak table acceleration. Thus, the isolated structure was shown to respond elastically to the El Centro signal having a peak table acceleration 7.65 times larger than that of the fixed base test and yet the peak base shear increased only 70%.

Uplift-Restrained Model

After the tests on the free-to-uplift structure were completed the corner bearings were replaced by bearings containing the uplift restrainer device. The model was then subjected to the same set of earthquake ground motions. The horizontal and vertical displacements which occurred at the corners of the structure (Figure 6.7) confirm that the restrainer device not only prevented the uplift seen previously but also essentially limited the relative horizontal displacement of the structure to the free displacement of the restrainer device. It is important to note (Figure 6.2) that uplift only occurred at times of peak lateral bearing displacement. This was always the case.

The peak story acceleration profiles were plotted for the tests on the uplift-restrained structure (Figure 6.8). For the shaking table inputs which did not cause the restrainer device to go into tension the profiles are similar in shape to the free-to-uplift profiles. The acceleration profiles for the Bucharest, Mexico City, and El Centro tests, which had peak table accelerations similar to those in the tests on the free-to-uplift model where uplift occurred, are different. The magnitude of the peak roof acceleration when the displacement control device was activated was larger; almost double for the El Centro signal, 60% higher for the Mexico signal, and about 20% higher for the Bucharest signal.

The profiles for the test structure isolated with and without the displacement control device are compared in Figure 6.9 for the El Centro input. This plot illustrates the increase in story acceleration, and consequently base shear, due to the action of the restrainer device.

The restrainers also reduced the magnitude of the vertical acceleration response (Figure 6.10) from that seen in the free-to-uplift test (Figure 6.3) by a factor of about 3. The effect of the restrainer on the shape of the axial and shear force hysteresis loops for the restrained bearings is seen in Figure 6.11. Both hysteresis loops are now stable and the shear loop reflects the bilinear stiffness properties due to the displacement control device.

To investigate the effect of the restrainer device on the higher modes of the structure the FFTs of the roof acceleration time histories were plotted for the Bucharest, Mexico City and El Centro tests on the free-to-uplift and restrained structure in Figure 6.12. There appears to be only a slight difference in the higher mode responses because of the device. At the lower magnitudes of input, when the device did not go into tension, there was no difference in the response of the structure.

7. CONCLUSIONS

Although earthquake simulator tests have been performed previously to evaluate base isolation systems, these studies were all performed on short stiff structures. Base isolation has not been proposed for taller buildings because of the obvious problems of column uplift and longer structure period.

The displacement control device described here successfully restrains columns from uplift during earthquake motions having magnitudes which previously caused column uplift in the unrestrained nine-story steel frame model. The device was installed within the hollow core of a multilayer elastomeric bearing and was placed under each corner column of the base isolated structure. The interior columns were supported by the same bearings without the displacement control device. The devices were set to allow only 2.25 inches of free horizontal displacement before they were fully extended, thereby limiting further horizontal displacement because of the increased stiffness of the system. The vertical component of force in the device served to restrain the column against uplift.

For earthquake tests during which the device extended fully, the maximum story accelerations were about double those for similar input signal magnitudes where the device had not been installed. The higher frequency responses of the structure were not increased at the times when the device was fully extended because of the smooth transition in the horizontal bearing stiffness.

While column uplift was the primary concern in the isolation tests on the nine-story steel frame, the uplift restrainer devices could clearly also be used for horizontal displacement control. The devices would act in this capacity as a fail-safe mechanism, and would be designed to come into effect only when the bearing displacement exceeded the maximum allowable displacement or the design displacement.

REFERENCES

[1] A. G. Tarics, "The Implementation of Base Isolation for the Foothill Communities Law and Justice Center" Report the the National Science Foundation and the County of San Bernardino, Reid and Tarics Associates, San Francisco, (1984).

[2] J. M. Kelly, K. E. Beucke and M. S. Skinner, "Experimental Testing of a Friction Damped Aseismic Base Isolation System with Fail-Safe Characteristics", Report No. UCB/EERC-80/18, Earthquake Engineering Research Center, University of California, Berkeley, (1980).

[3] Arthur A. Huckelbridge, "Earthquake Simulation Tests of a Nine Story Steel Frame with Columns Allowed to Uplift" Report No. UCB/EERC-77/23, Earthquake Engineering Research Center, University of California, Berkeley, (1977).

[4] R. Sause and V. V. Bertero, "A Transducer for Measuring the Internal Forces in the Columns of a Frame-Wall Reinforced Concrete Structure" Report No. UCB/EERC-83/05, Earthquake Engineering Research Center, University of California, (1983).

[5] "Natural Rubber Engineering Data Sheets", Malaysian Rubber Producers Research Association, Hertford, England.

[6] Earthquake Catalog of California, January 1, 1900 to December 31, 1974, Charles R. Read et. al., California Division of Mines and Geology, Special Publication No. 52, 1st Edition and Cal. Tech. Report No., EERL 80-01, D.M. Lee, P.C. Jennings, G.W. Housner, (January 1980).

[7] The Romanian Earthquake of March 4, 1977. Preliminary Report of UNESCO Earthquake reconnaissance mission, Ambraseys N., (April 1977).

[8] An Investigation of the Miyagi-Ken-Oki, Japan, Earthquake of June 12, 1978, Nat. Bureau of Standards Center for Building Technology, Washington, D.C., Bruce R. Ellingwood (Ed), (October 1980).

[9] The Mexico Earthquake of September 19, 1985, A Preliminary Report, The John A. Blume Earthquake Engineering Center, Dept. of Civil Engineering, Stanford University, Rept. NO.77, Shigeru Suzuki and Anne S. Kiremidjian, (January 1986).

[10] J. M. Kelly and M. C. Griffith, "Base Isolation for Reinforced Concrete Structures", Paper presented at the ASCE Structures Conference, Orlando, Florida, (August 1987).

APPENDIX

A. MECHANICAL CONTROL DEVICE IN BEARING

The following analysis establishes a relation between shear force and horizontal displacement for a bearing containing the uplift restrainer device. The theory assumes linear elastic material behavior and is based on the following variables (Fig. A.1),

H = total height of bearing

B = width of bearing

L = length of restrainer device when $P = 0^+$

P = axial force in the restrainer device

F_x = shear force applied to the bearing

W = axial dead load on bearing

k_v = vertical bearing stiffness

k_h = horizontal bearing stiffness

k_d = axial stiffness of restrainer device

u_x = horizontal displacement of bearing

u_y = vertical displacement of bearing due to P

u_d = horizontal displacement of bearing when $P = 0^+$

u_L = axial displacement of restrainer device

δ_y = decrease in height of bearing due to W

$h = H - ($ thickness of top and bottom plates $+ \delta_y)$

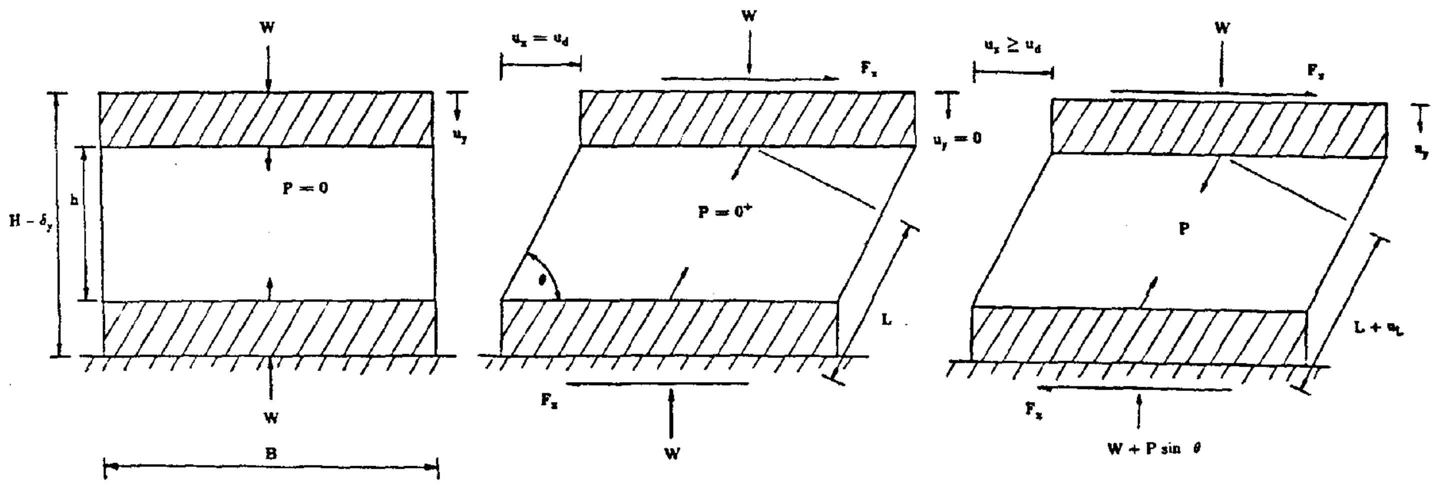

Figure A.1

Based on the kinematics of the restrainer device, the following relationships can be written :

$$\sin\theta = \frac{h - u_y}{L + u_L} \quad , \quad \cos\theta = \frac{u_x}{L + u_L} \quad \text{and} \tag{A.1}$$

$$(L + u_L)^2 = u_x^2 + (h - u_y)^2 \ ; \tag{A.2}$$

and, from equilibrium,

$$F_x = k_h \, u_x + P \cos\theta \tag{A.3}$$

$$F_y = P \sin\theta = k_v \, u_y \tag{A.4}$$

$$P = k_d \, u_L \ . \tag{A.5}$$

Expanding equation A.2 and assuming $u_L << L$ and $u_y << h$ yields

$$L^2 + 2Lu_L = u_x^2 + h^2 - 2hu_y \quad , \tag{A.6}$$

from which

$$u_y = \frac{u_x^2 + h^2 - L^2}{2\,h} - \frac{L}{h}\,u_L \quad . \tag{A.7}$$

Substituting for u_L using equation A.5 gives

$$u_y = \frac{u_x^2 + h^2 - L^2}{2\,h} - \frac{L}{h}\,\frac{P}{k_d} \quad , \tag{A.8}$$

and eliminating u_y from equation A.4,

$$P\sin\theta = k_v\,u_y = k_v\left[\frac{u_x^2 + h^2 - L^2}{2\,h}\right] - \frac{L}{h}\,\frac{k_v}{k_d}\,P \quad .$$

Therefore,

$$P\left[\sin\theta + \frac{L}{h}\,\frac{k_v}{k_d}\right] = k_v\left[\frac{u_x^2 + h^2 - L^2}{2\,h}\right]$$

and

$$P = \frac{k_v(\,u_x^2 + h^2 - L^2\,)}{2\,h\,(\,\sin\theta + \frac{L}{h}\,\frac{k_v}{k_d}\,)} \quad . \tag{A.9}$$

Equation A.9 can be substituted into equation A.3 to give

$$F_x = k_h\,u_x + \frac{k_v\,(\,u_x^2 + h^2 - L^2\,)}{2\,h\,(\,\sin\theta + \frac{k_v}{k_d}\,\frac{L}{h})}\cos\theta \quad . \tag{A.10}$$

Assuming that $u_L << L$ and $u_y << h$, the expressions for $\sin\theta$ and $\cos\theta$ reduce to

$$\sin\theta \approx \frac{h}{L} \quad \text{and} \quad \cos\theta \approx \frac{u_x}{L} \quad , \tag{A.11}$$

so that, from equation A.10,

$$F_x = k_h\, u_x + \frac{k_v\,(\,u_x^2 + h^2 - L^2\,)}{2\,h\,(\,\frac{h}{L} + \frac{L}{h}\,\frac{k_v}{k_d})}\,\frac{u_x}{L}$$

$$= k_h\, u_x + \frac{k_v\,(\,u_x^2 + h^2 - L^2\,)}{2\,h^2\,(\,1 + \frac{L^2}{h^2}\,\frac{k_v}{k_d}\,)}\,u_x\ . \tag{A.12}$$

Now, defining $u_x = u_d + e_x$ and noting that $u_d^2 = L^2 - h^2$, equation A.12 gives

$$F_x = k_h\,(\,u_d + e_x\,) + \left[\frac{k_v\,(\,u_d^2 + 2\,u_d\,e_x + e_x^2 + h^2 - L^2\,)}{2\,h^2\,(\,1 + \frac{L^2}{h^2}\,\frac{k_v}{k_d})}\right](\,u_d + e_x\,)$$

$$= k_h\,u_d + \left[k_h + \frac{k_v\,u_d^2}{h^2 + L^2\,\frac{k_v}{k_d}}\right] e_x + O(e_x)^2 \quad \text{terms}\ . \tag{A.13}$$

Thus, to the first order,

$$F_x = k_h\,u_d + \left[k_h + \frac{k_v\,u_d^2}{h^2 + L^2\,\frac{k_v}{k_d}}\right] e_x \tag{A.14}$$

when $u_x \geq u_d$.

When $u_x \leq u_d$, the expression for F_x is simply

$$F_x = k_h \, u_x \tag{A.15}$$

since the restrainer device carries no axial load (P) at these displacements.

TABLES

SYMBOL	EARTHQUAKE	DATE	PGA (g)
ec1,ec2	Imperial Valley, Calif. El Centro Site	May 18,1940 S00E	0.35
taft1,taft2	Kern County, Calif. Taft Lincoln School Tunnel	July 21,1952 S69E	0.18
sf1,sf2	San Francisco, Calif. Golden Gate Park	March 22,1957 S80E	0.10
park1,park2	Parkfield, Calif. Cholame,Shandon,CA array #2	June 27,1966 N65E	0.49
pac1,pac2	San Fernando, Calif. Pacoima Dam Site	February 9,1971 S14W	1.08
miyagi	Miyagi-Ken-Oki Tohoku University	June 12th 1978 S00E	0.24
buc1	Bucharest Building Research Inst.	March 7th, 1977 EW	0.21
mex2m,sct	Mexico City SCT Site	September 19, 1985 S60E	0.20

Table 5.1 Earthquake Signals Used in Testing Program

Note: If the symbol for the earthquake includes a suffix of "1" then no additional filtering was applied to the signal. A suffix of "2" means that the real-time signal was high-pass filtered at 0.1 Hz. For example, "ec1" is unfiltered, "ec2" was high-pass filtered.

PARAMETER	1/4-SCALE MODEL/PROTOTYPE	
Length	L	1/4
Time	$\sqrt{L}$	1/2
Mass	L^2	1/16
Displacement	L	1/4
Acceleration	1	1/1
Stress	1	1/1
Strain	1	1/1
Force	L^2	1/16
Area	L^2	1/16

Table 5.2 Similitude Scale Factors for Prototype Responses

FILE NO.	RUN	SPAN	PK. TABLE ACCEL. (g)	PK. MODEL ACCEL. (g)	REL. BEARING DISPL. (in.)	UPLIFT (Y/N)
860707.01	$\sqrt{4}$ ec2	150	.296	.258	.806	N
860707.02	$\sqrt{4}$ miyagi	200	.174	.220	.930	N
860707.03	$\sqrt{4}$ taft2	220	.428	.334	1.048	N
860707.04	$\sqrt{4}$ pac2	220	.338	.290	1.252	N
860707.05	$\sqrt{4}$ park2	220	.243	.226	1.105	N
860707.06	$\sqrt{4}$ sf2	230	1.411	.467	1.183	N
860707.07	$\sqrt{4}$ buc1	300	.199	.242	1.348	N
860707.08	$\sqrt{4}$ mex2m	150	.173	.231	1.317	N
860707.09	$\sqrt{4}$ mex2m	200	.191	.325	2.337	N
860707.10	$\sqrt{4}$ buc1	275	.251	.323	2.207	N
860707.11	$\sqrt{4}$ sf2	300	1.590	.488	1.519	N
860707.12	$\sqrt{4}$ park2	350	.425	.337	1.942	N
860707.13	$\sqrt{4}$ pac2	350	.562	.463	1.985	N
860707.14	$\sqrt{4}$ taft2	400	.848	.407	2.259	N
860707.15	$\sqrt{4}$ miyagi	400	.310	.343	2.404	N
860707.16	$\sqrt{4}$ ec2	300	.633	.463	2.797	Y
860707.17	$\sqrt{4}$ ec2	150	.338	.202	.991	N
860708.03	$\sqrt{4}$ ec2	150	.313	.244	.904	N
860708.04	$\sqrt{4}$ ec2	225	.460	.288	1.712	N
860708.05	$\sqrt{4}$ ec2	300	.604	.453	2.648	Y
860708.06	$\sqrt{4}$ ec2	400	.842	.607	3.784	Y
860708.07	$\sqrt{4}$ ec2	150	.328	.205	1.014	N
860709.01	$\sqrt{4}$ buc1	275	.241	.293	1.825	N
860709.02	$\sqrt{4}$ buc1	350	.296	.444	2.729	Y
860709.03	$\sqrt{4}$ buc1	400	.343	.537	3.259	Y
860709.04	$\sqrt{4}$ mex2m	175	.146	.254	1.898	N
860709.05	$\sqrt{4}$ mex2m	250	.194	.425	3.063	N
860709.06	$\sqrt{4}$ mex2m	275	.219	.586	3.372	Y
860709.07	$\sqrt{4}$ mex2m	275	.217	.520	3.416	Y
860709.08	$\sqrt{4}$ buc1	400	.348	.767	3.723	Y
860709.09	$\sqrt{4}$ ec2	375	.723	.579	3.603	Y
860709.10	$\sqrt{4}$ ec2	150	.353	.213	1.054	N

Table 5.3 Maximum Model Responses on Bearings without Displacement Control Device

FILE NO.	RUN	SPAN	PK. TABLE ACCEL. (g)	PK. MODEL ACCEL. (g)	REL. BEARING DISPL. (in.)	UPLIFT (Y/N)
860711.03	$\sqrt{4}$ ec2	150	.336	.279	.637	N
860711.04	$\sqrt{4}$ ec2	225	.487	.341	1.150	N
860711.05	$\sqrt{4}$ ec2	225	.420	.372	1.313	N
860711.06	$\sqrt{4}$ ec2	300	.627	.503	1.930	N
860711.07	$\sqrt{4}$ ec2	350	.726	.727	2.451	N
860711.08	$\sqrt{4}$ ec2	400	.832	.851	2.958	N
860711.09	$\sqrt{4}$ buc1	400	.351	.620	2.854	N
860711.10	$\sqrt{4}$ set	275	.168	1.524	3.635	N

Table 5.4 Maximum Model Responses on Bearings with Displacement Control Device

FIGURES

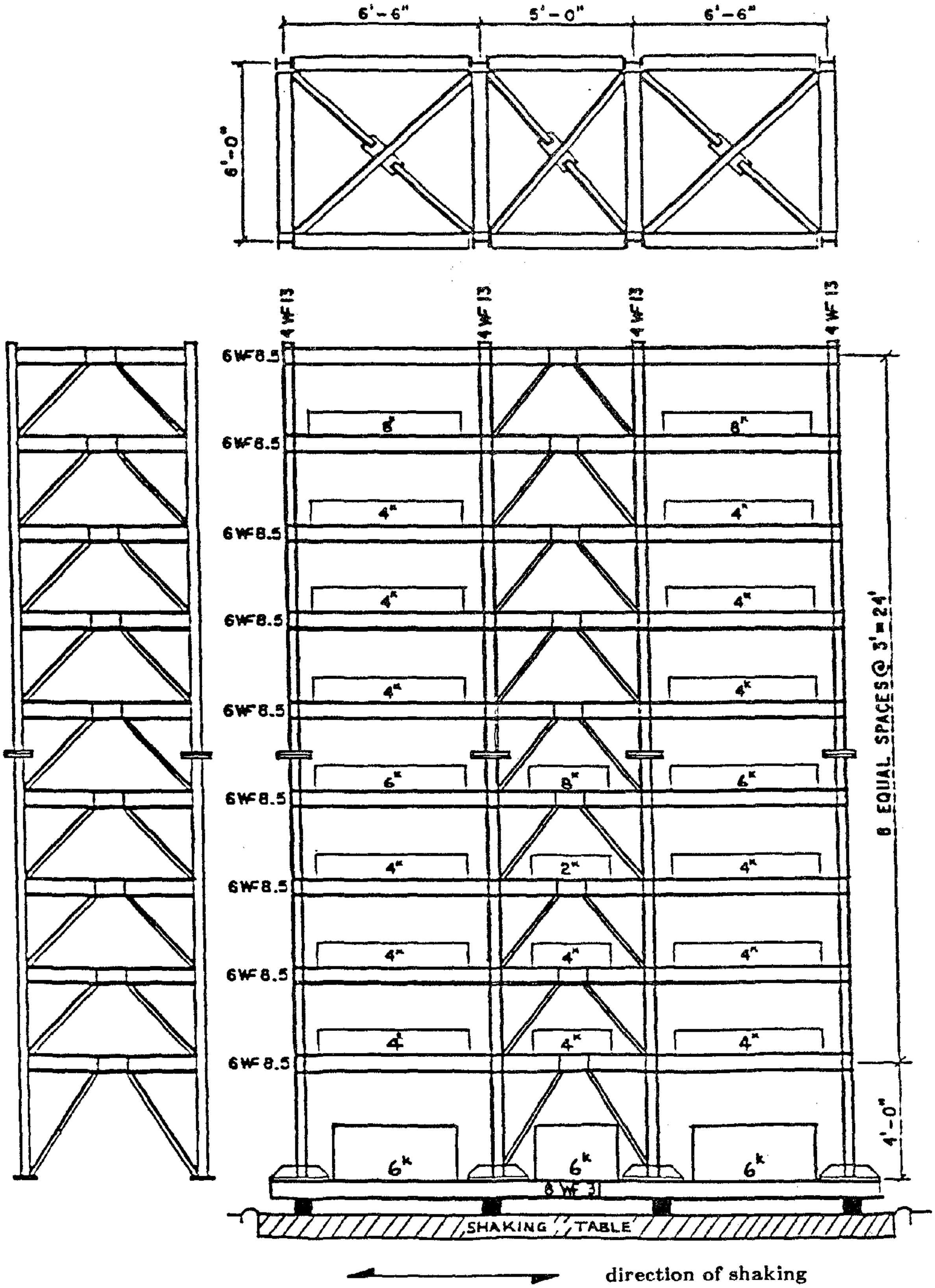

FIGURE 2.1 NINE STORY STEEL TEST FRAME

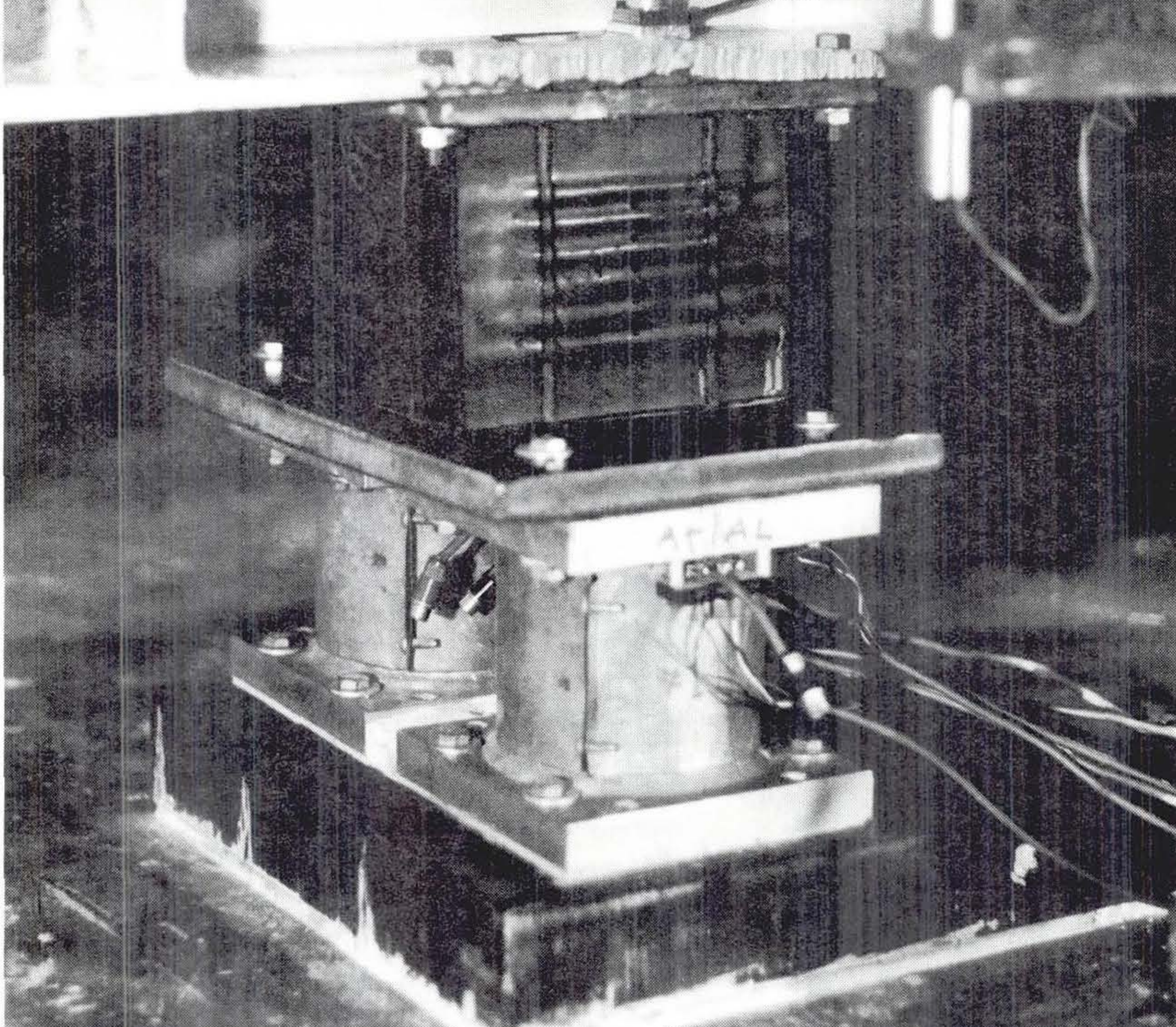

FIGURE 2.2 FORCE TRANSDUCER AND BEARING

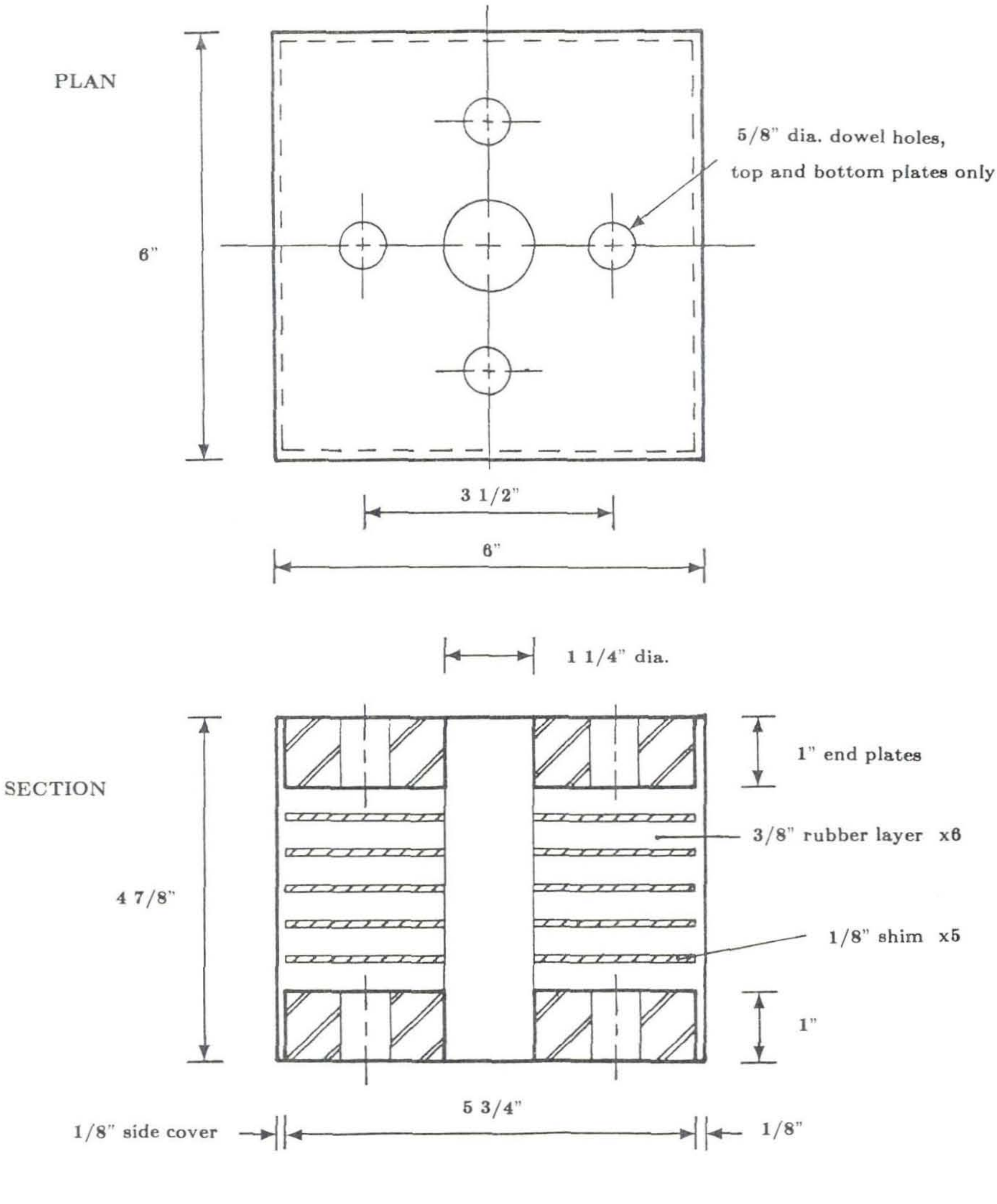

FIGURE 3.1 LEAD PLUG BEARING DETAILS

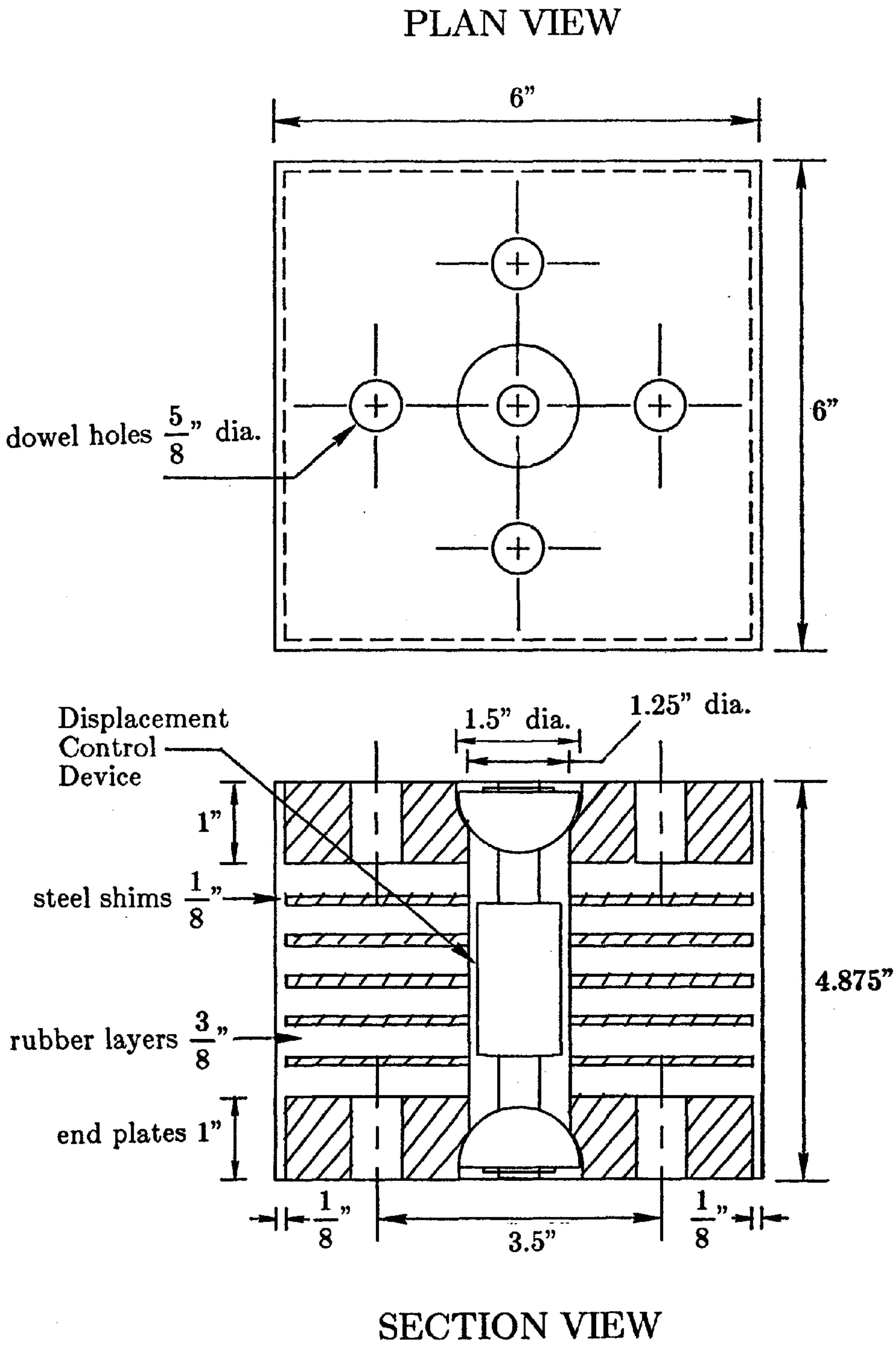

FIGURE 3.2 BEARING MODIFIED TO ACCEPT DISPLACEMENT CONTROL DEVICE

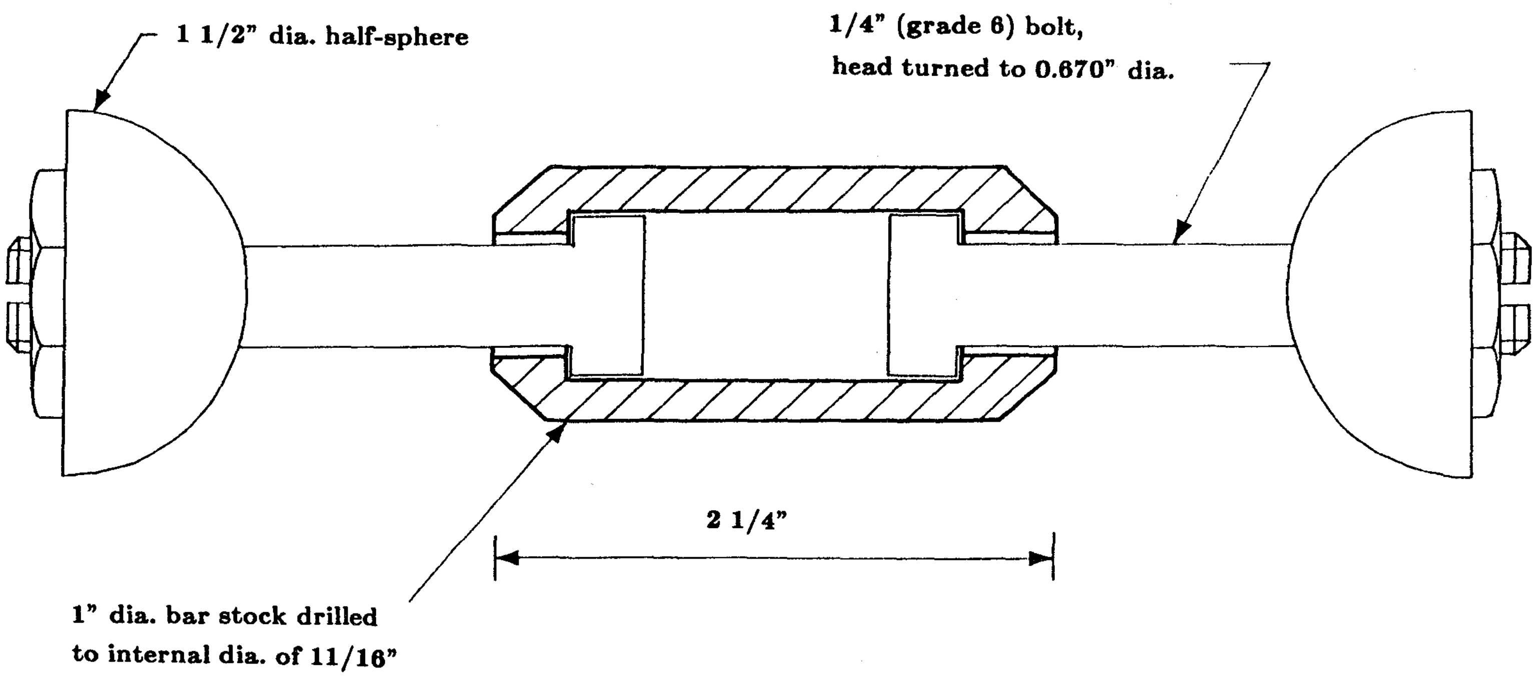

— travel adjustable

— shown fully extended

— tension capacity approx. 20 kips

FIGURE 3.3 DISPLACEMENT CONTROL DEVICE

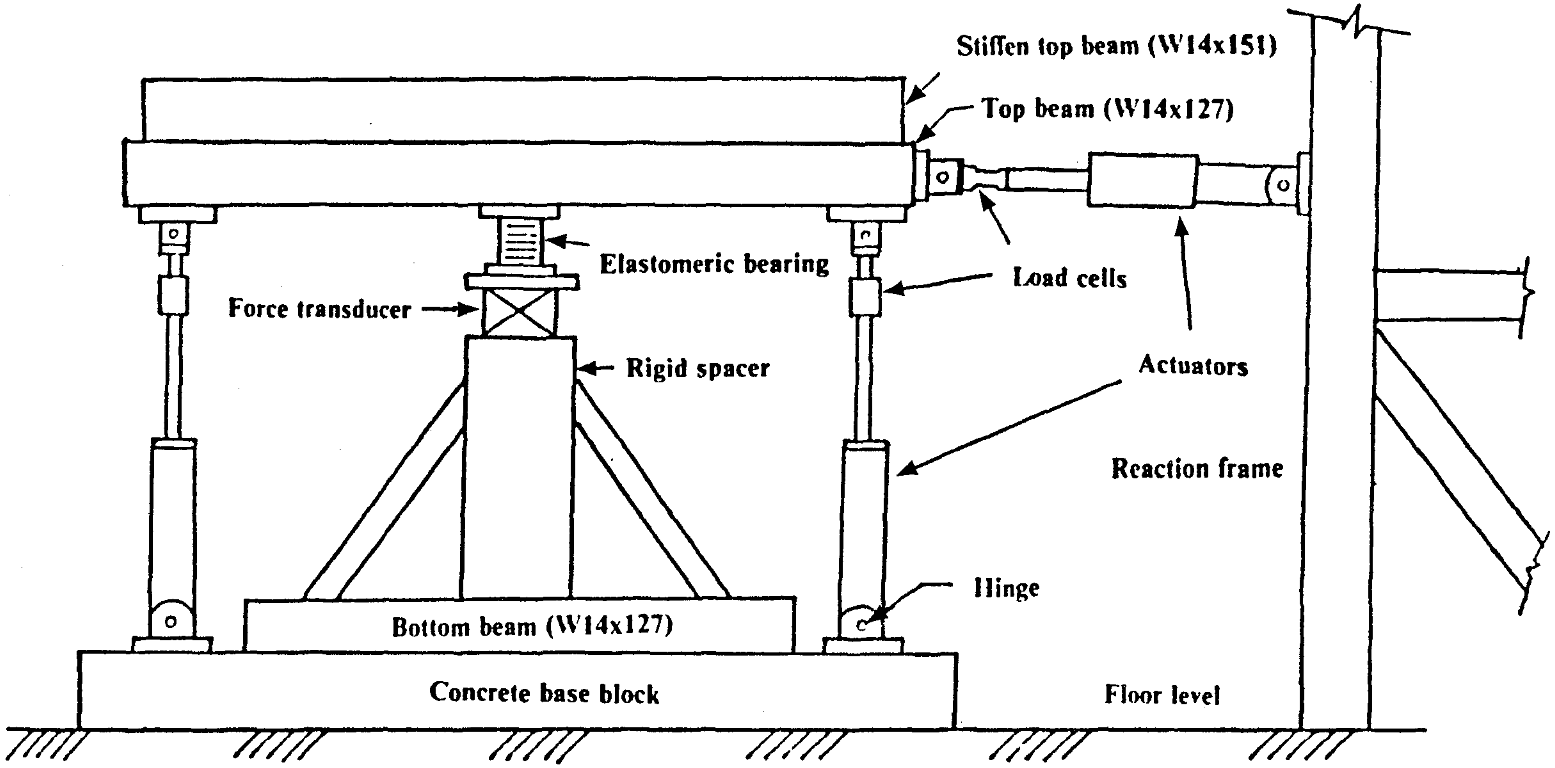

FIGURE 4.1 BEARING SHEAR TEST APPARATUS

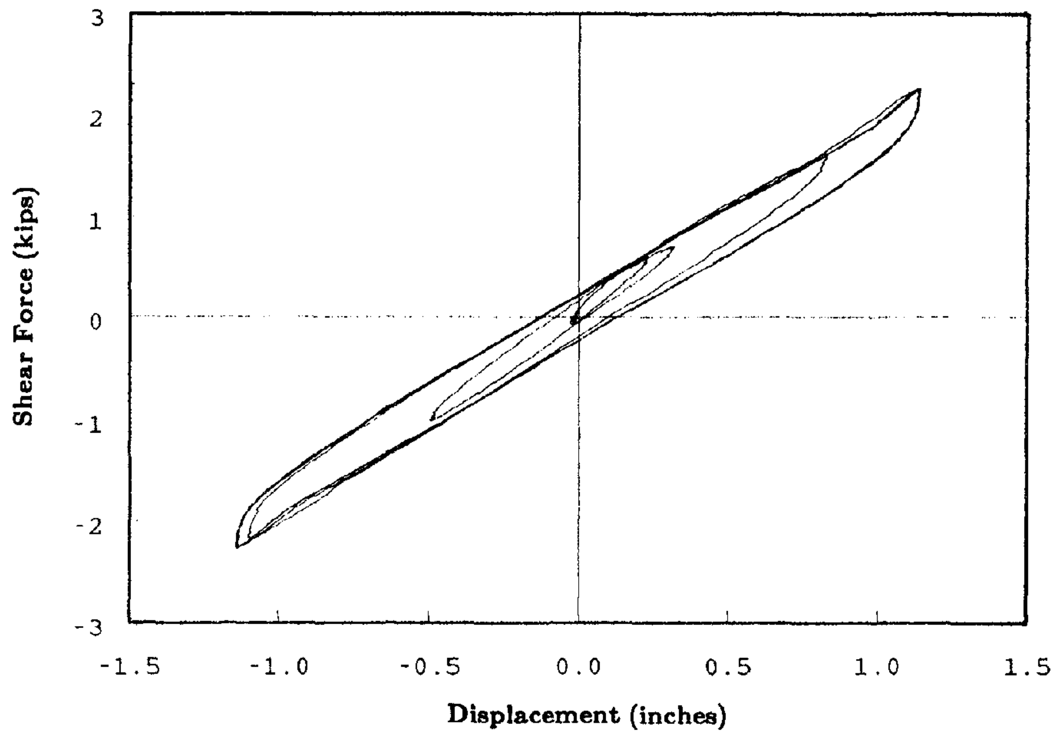

(a) Displacement amplitude less than u_d (device not activated)

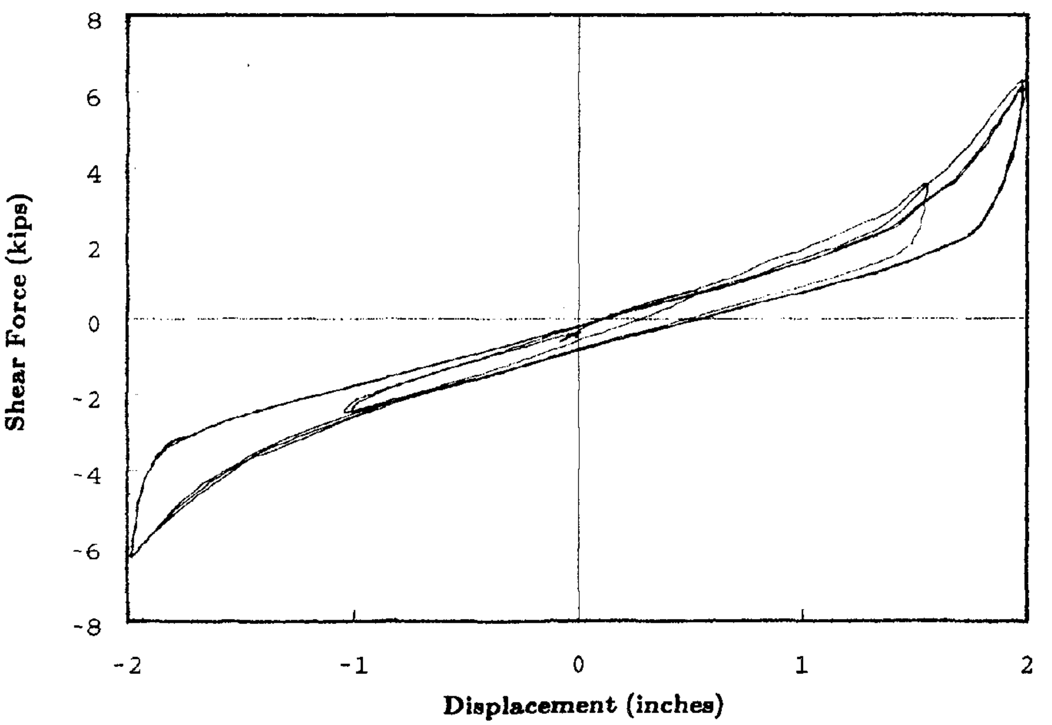

(b) Displacement amplitude greater than u_d (device activated)

FIGURE 4.2 SHEAR FORCE VS. DISPLACEMENT FOR RESTRAINED BEARING SUBJECTED TO SINUSOIDAL LOADING

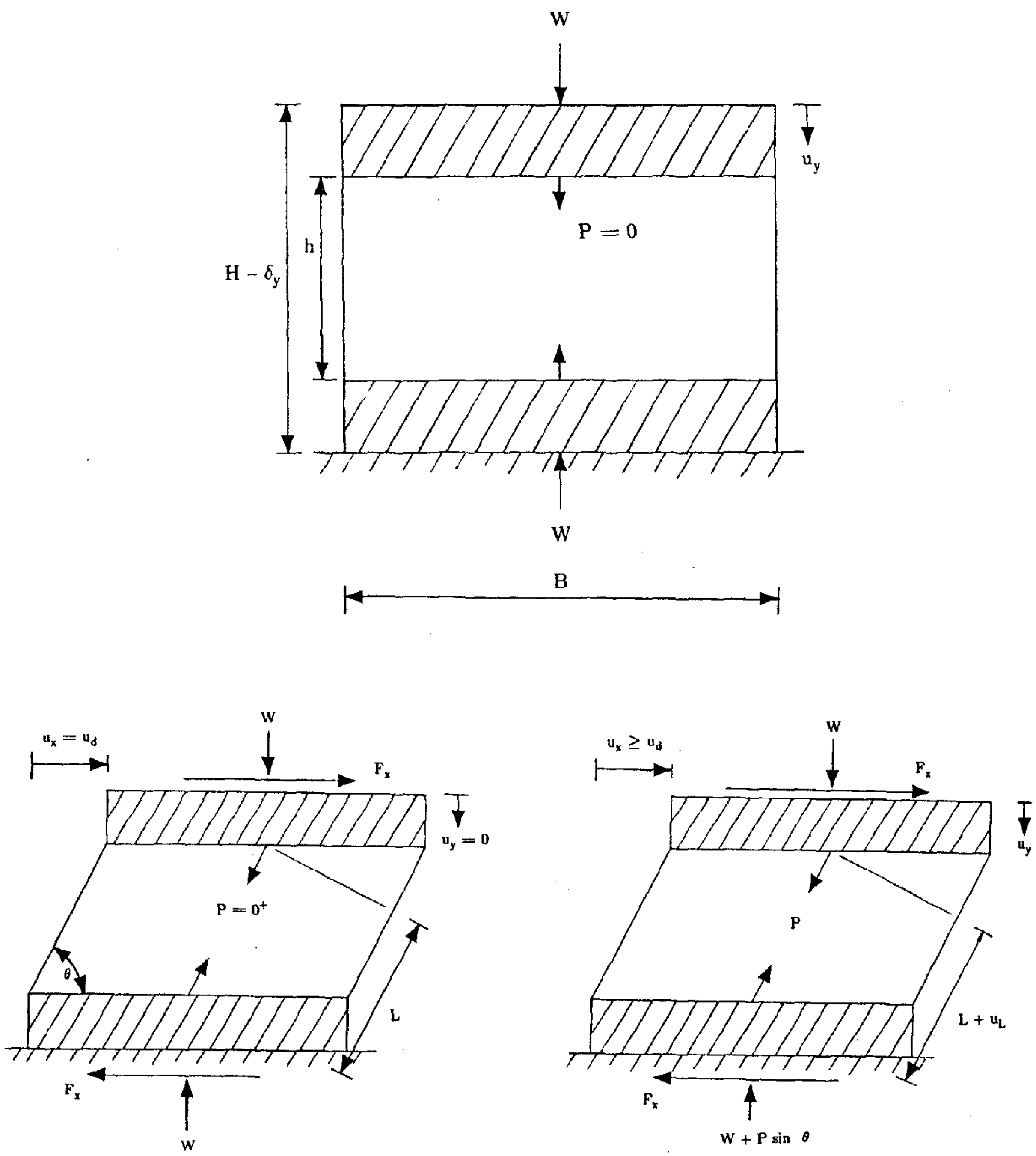

FIGURE 4.3 RESTRAINER BEARING FORCE DIAGRAM

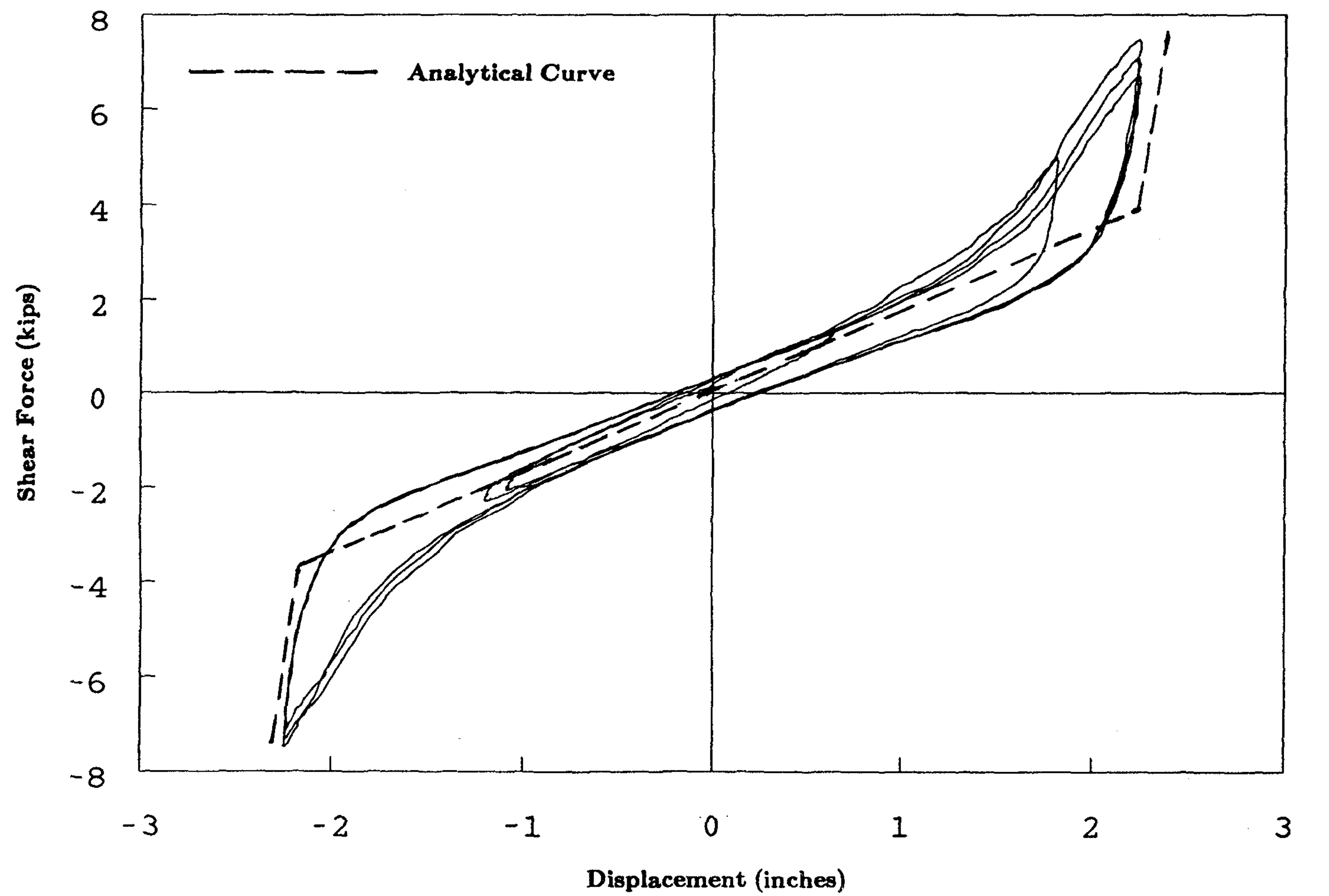

FIGURE 4.4 EXPERIMENTAL AND PREDICTED FORCE-DISPLACEMENT CURVES FOR RESTRAINED BEARING

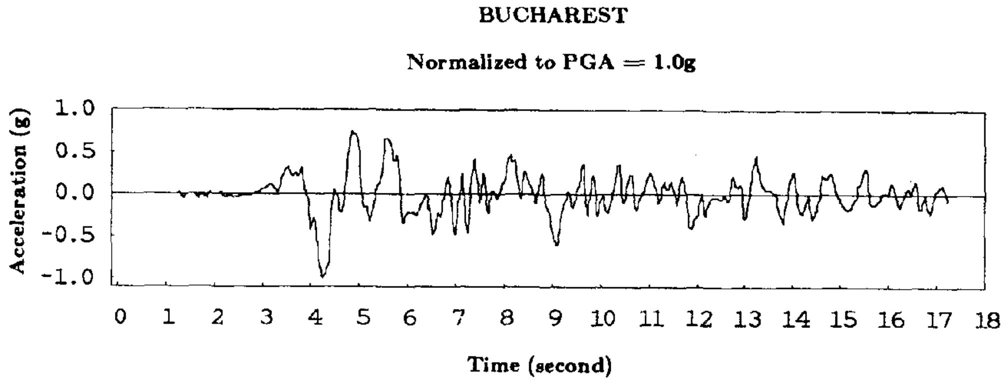

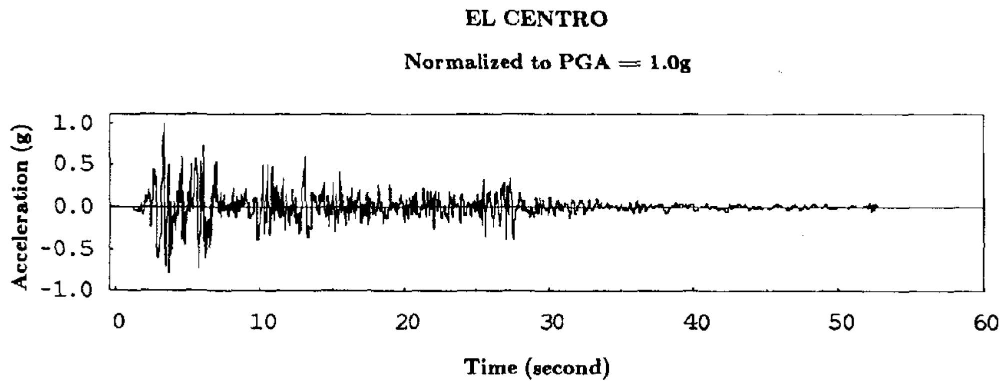

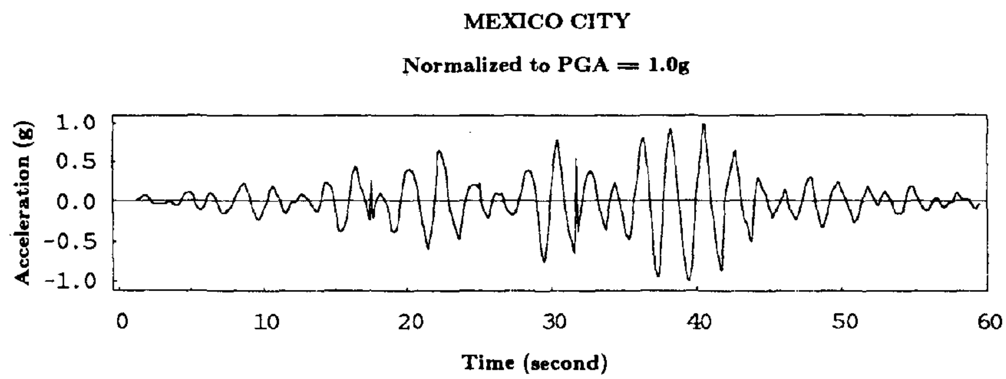

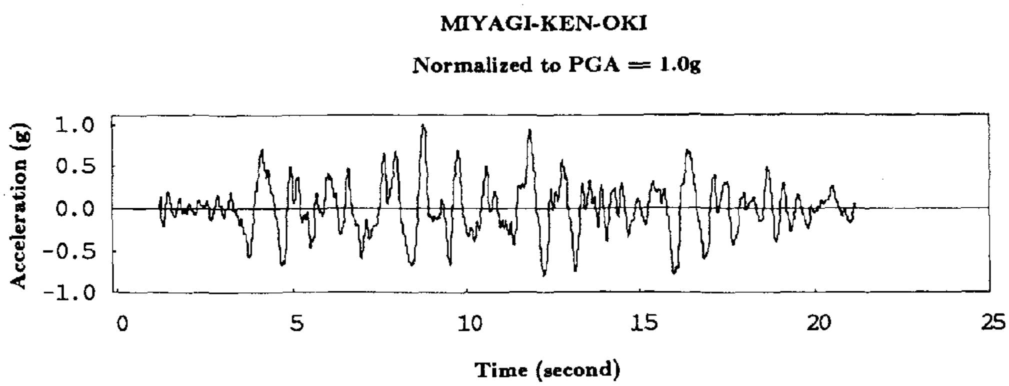

FIGURE 5.1 NORMALIZED EARTHQUAKE TABLE ACCELERATIONS

PACOIMA DAM

Normalized to PGA = 1.0g

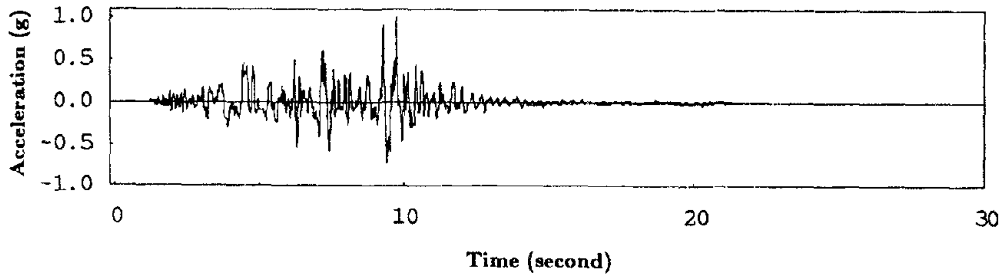

PARKFIELD

Normalized to PGA = 1.0g

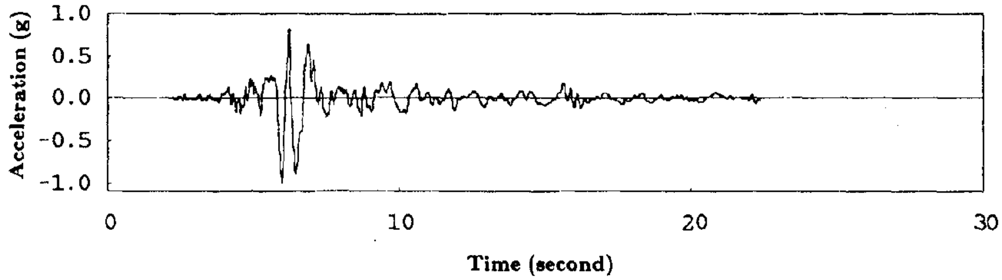

SAN FRANCISCO

Normalized to PGA = 1.0g

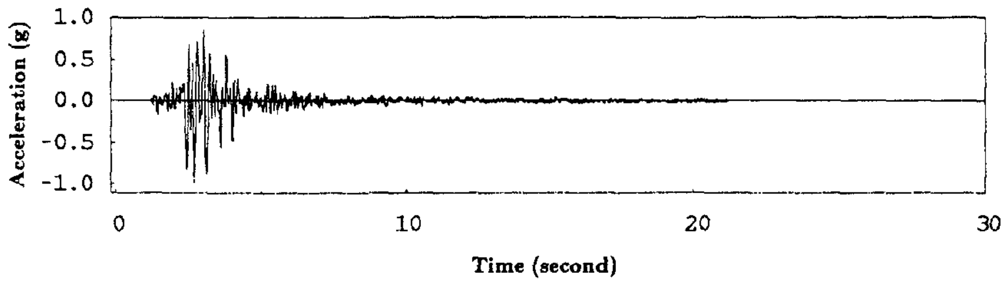

TAFT

Normalized to PGA = 1.0g

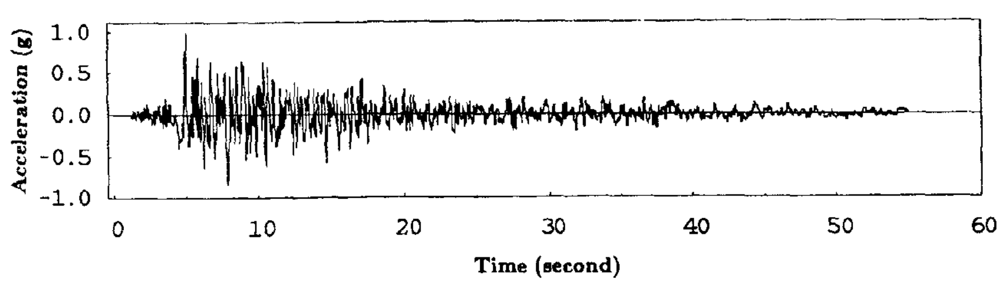

FIGURE 5.1 (continued)

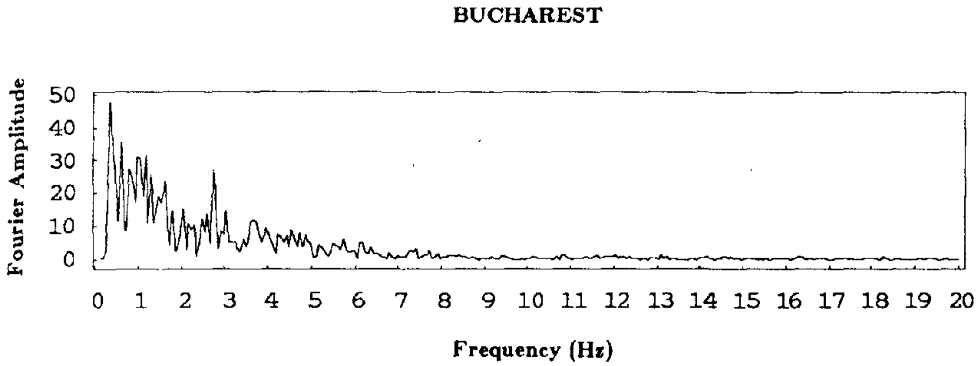

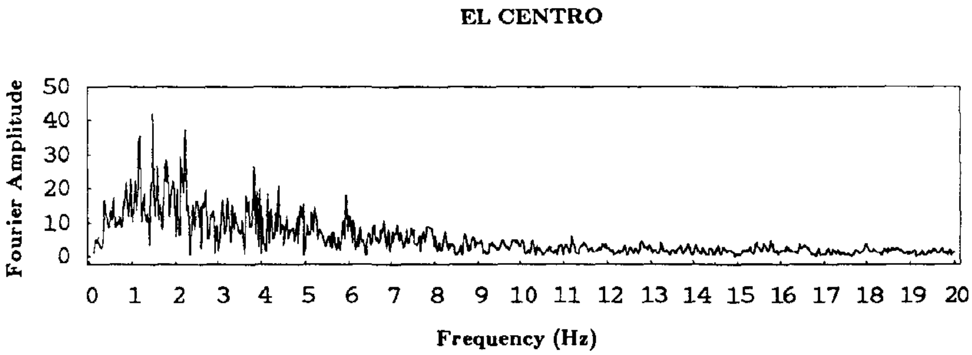

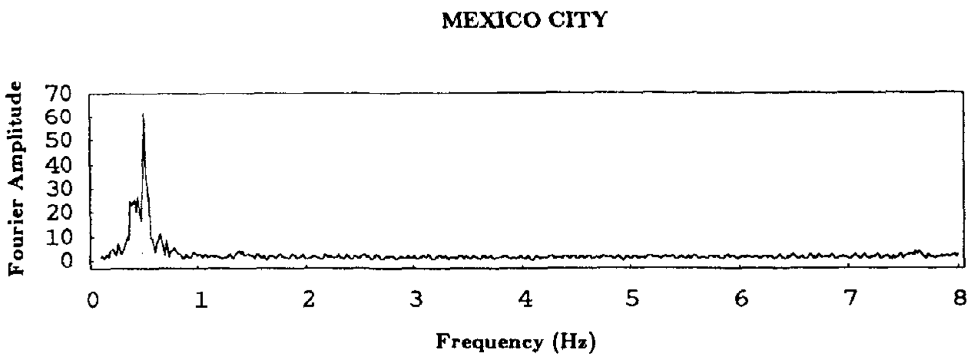

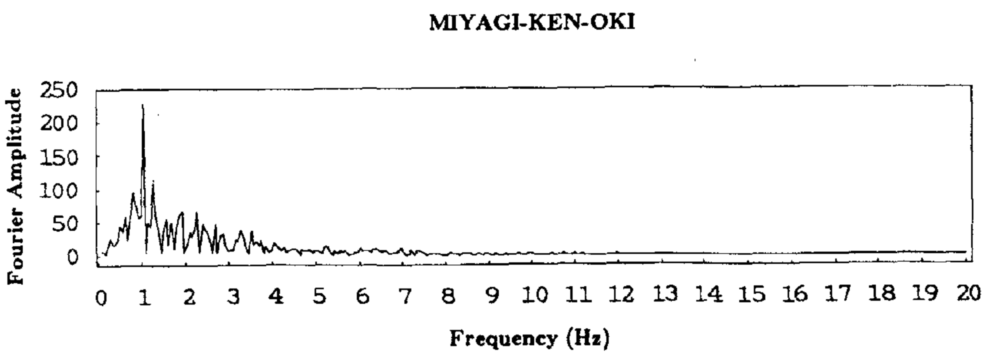

FIGURE 5.2 FFTS OF EARTHQUAKE TABLE ACCELERATIONS

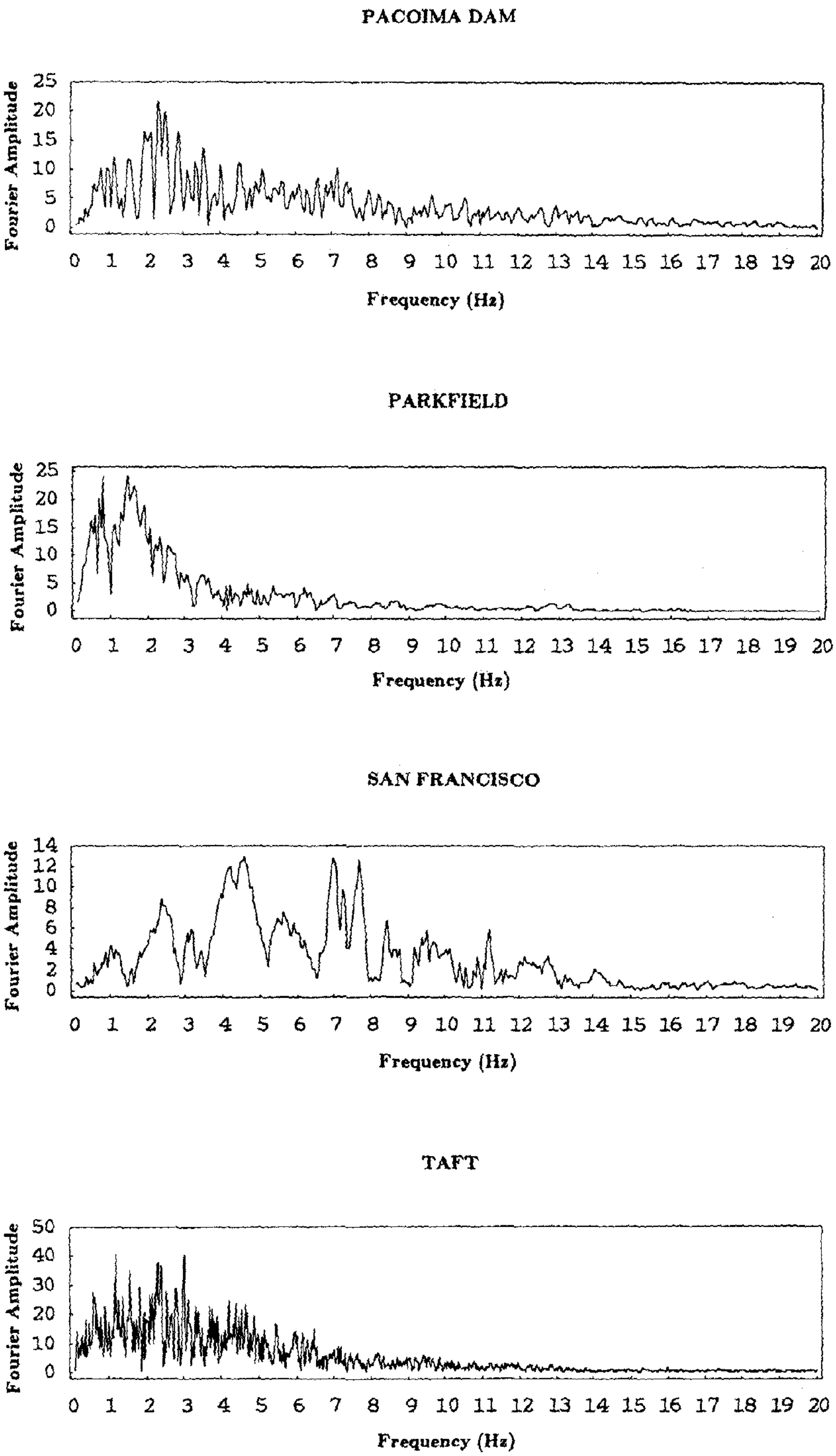

FIGURE 5.2 (continued)

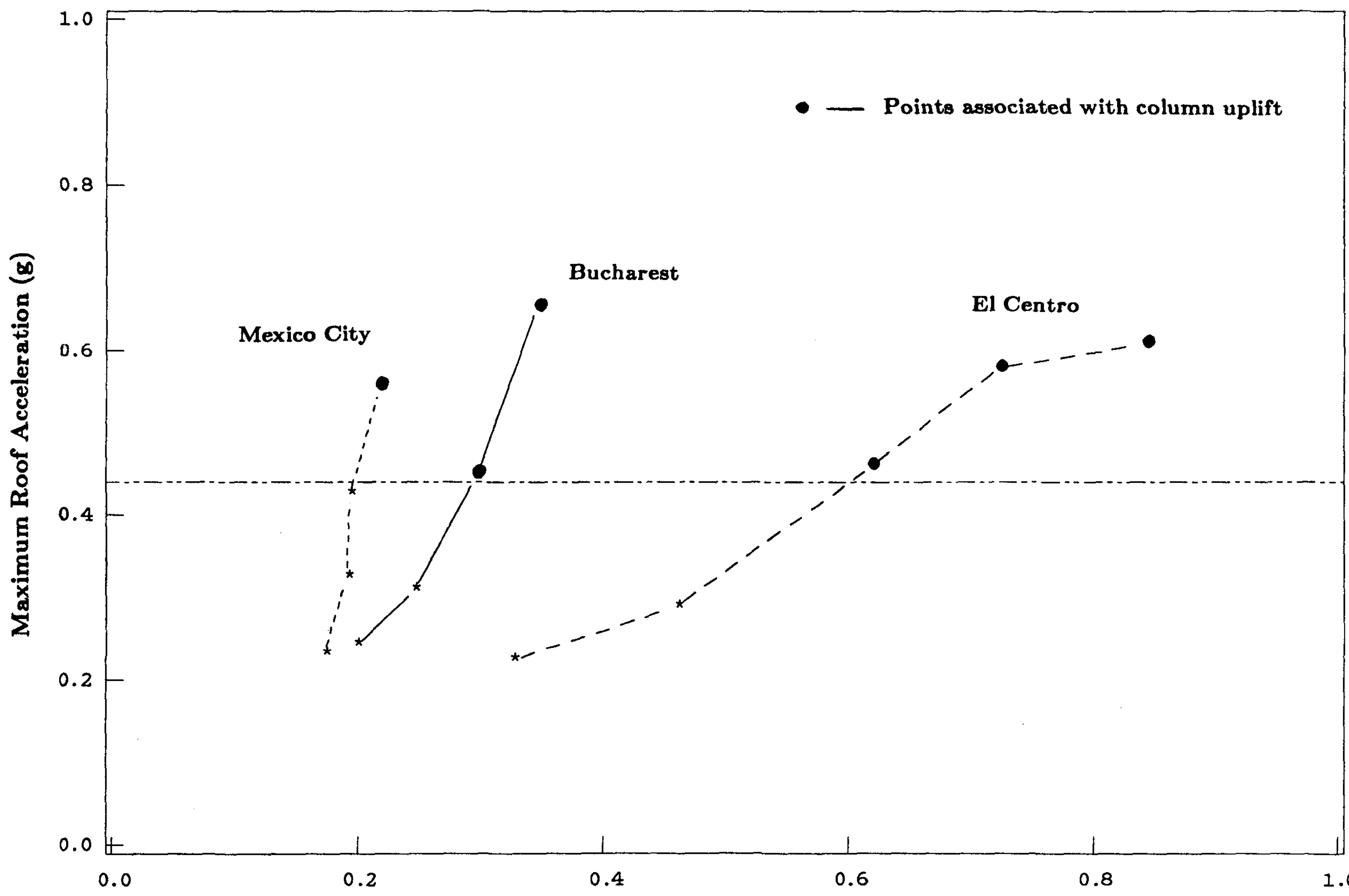

FIGURE 6.1 MAXIMUM ROOF ACCELERATION VS. MAXIMUM TABLE ACCELERATION FOR FREE-TO-UPLIFT MODEL

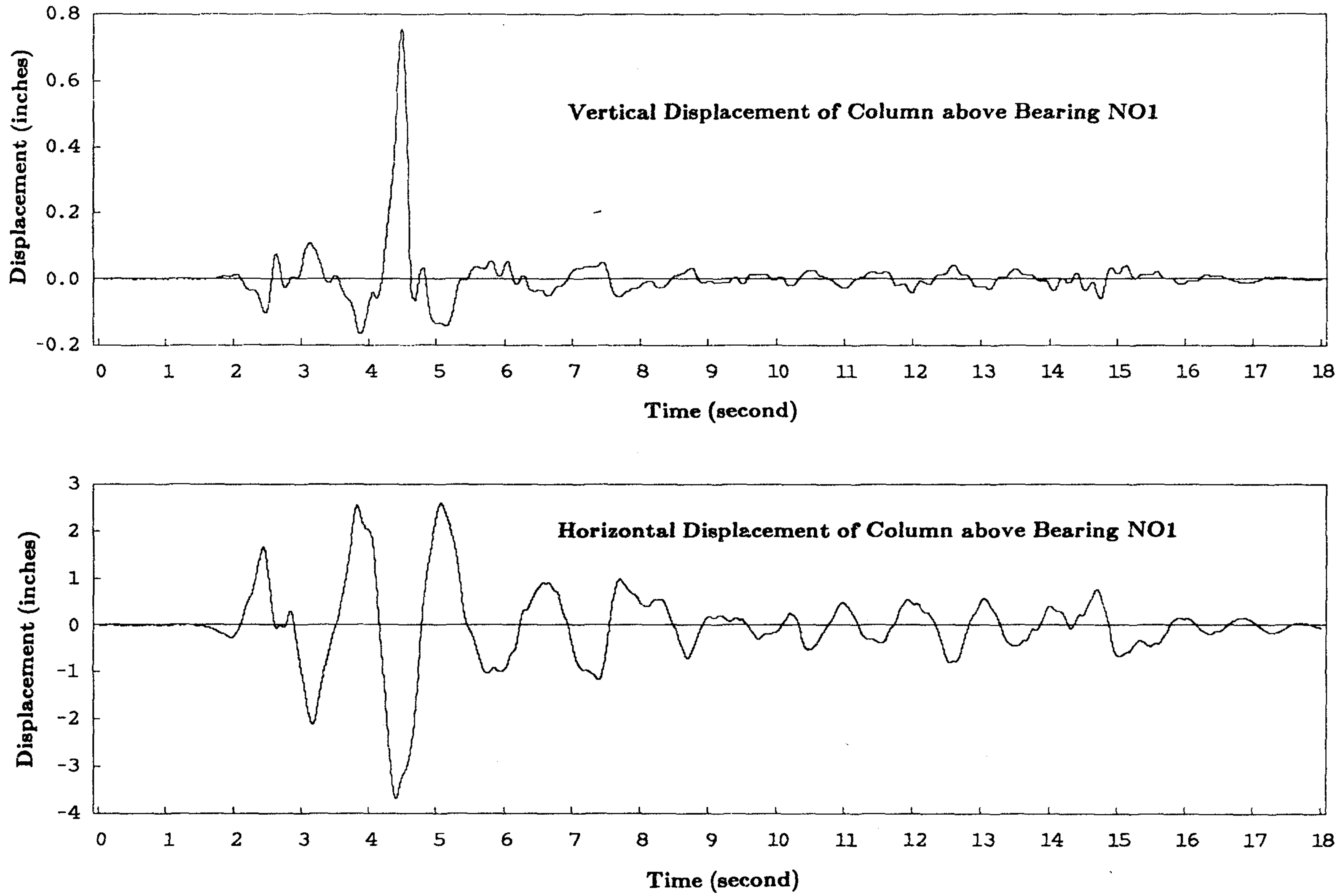

FIGURE 6.2 BEARING HORIZONTAL DISPLACEMENT AND COLUMN VERTICAL DISPLACEMENT DURING EL CENTRO-0.842g TEST (FREE-TO-UPLIFT CONDITION)

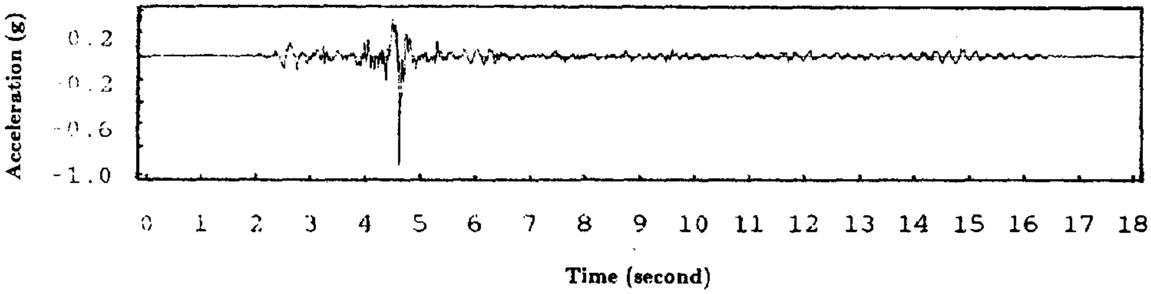

(a) Vertical Acceleration above Bearing NO1

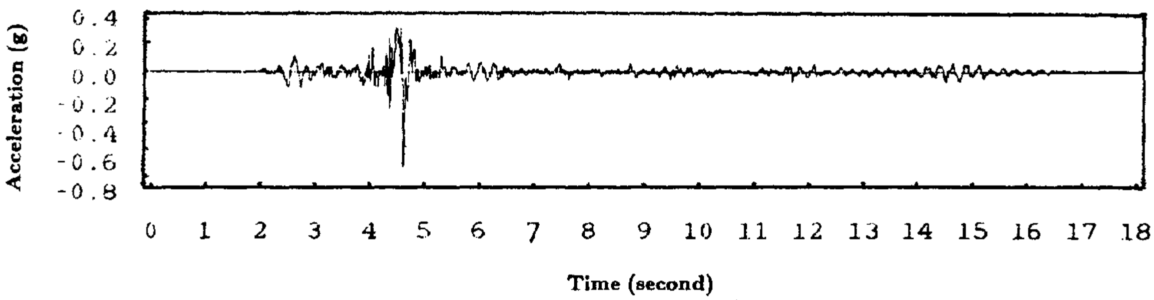

(b) Vertical Acceleration above Bearing NO2

FIGURE 6.3 VERTICAL ACCELERATIONS IN FREE-TO-UPLIFT MODEL DURING EL CENTRO-0.842g TEST

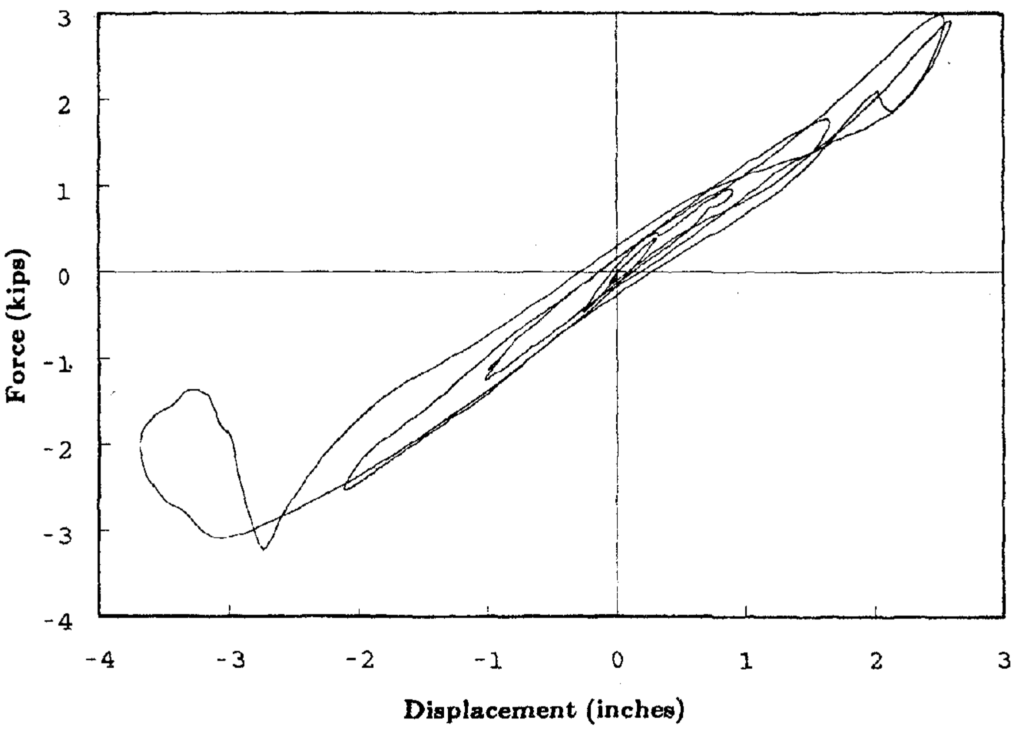

(a) Shear Force vs. Horizontal Displacement

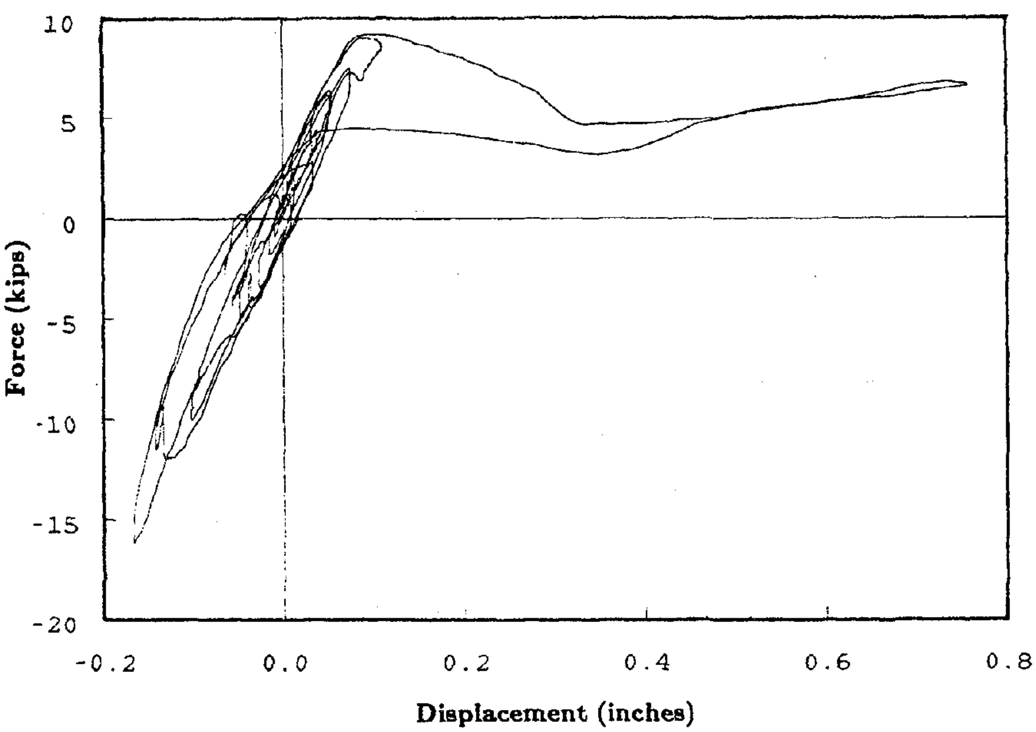

(b) Axial Force vs. Vertical Displacement

FIGURE 6.4 SHEAR AND AXIAL FORCE BEHAVIOR OF BEARINGS IN FREE-TO-UPLIFT CONDITION DURING EL CENTRO-0.842g TEST

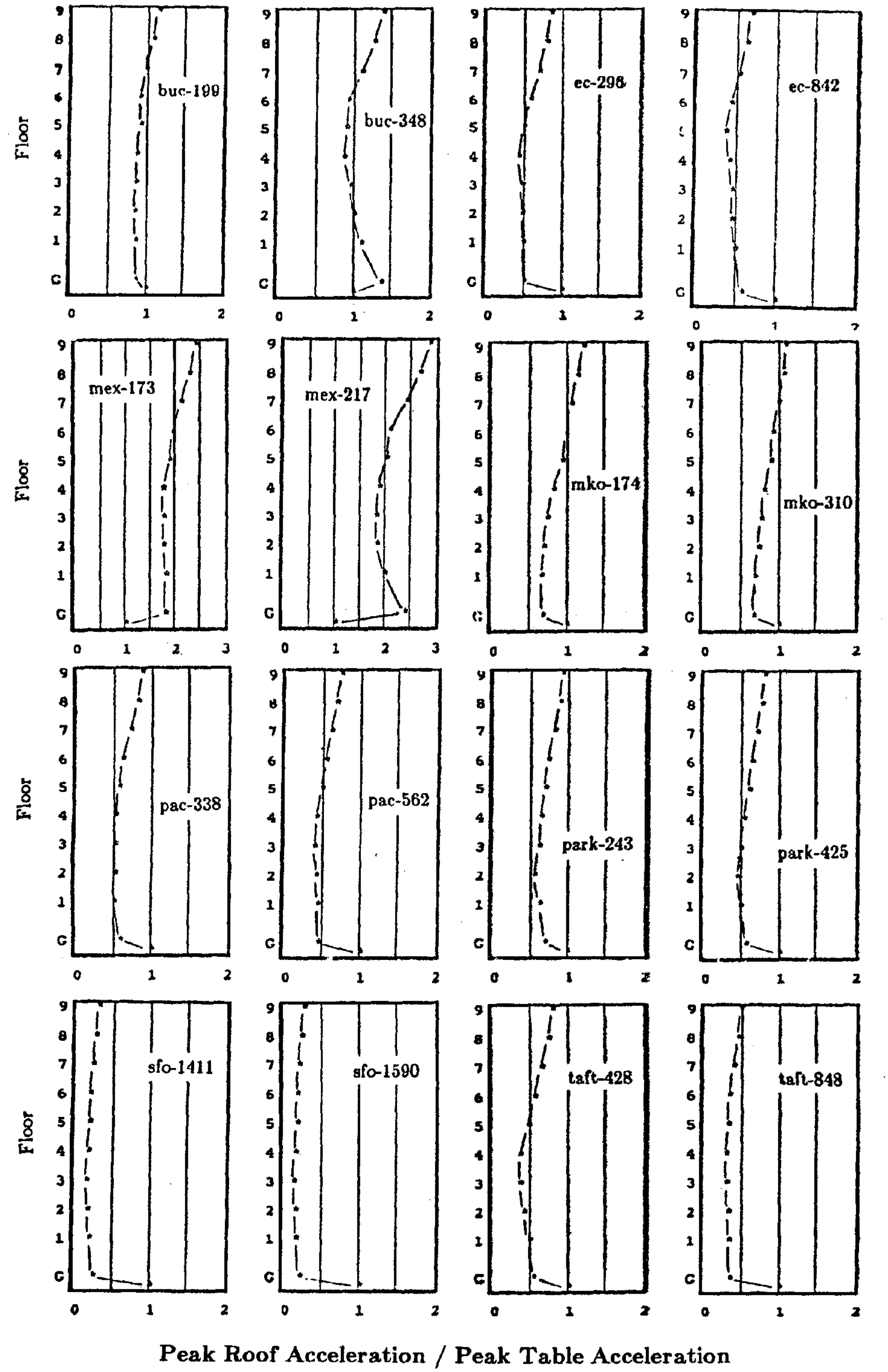

FIGURE 6.5 MAXIMUM STORY ACCELERATION PROFILES FOR FREE-TO-UPLIFT MODEL

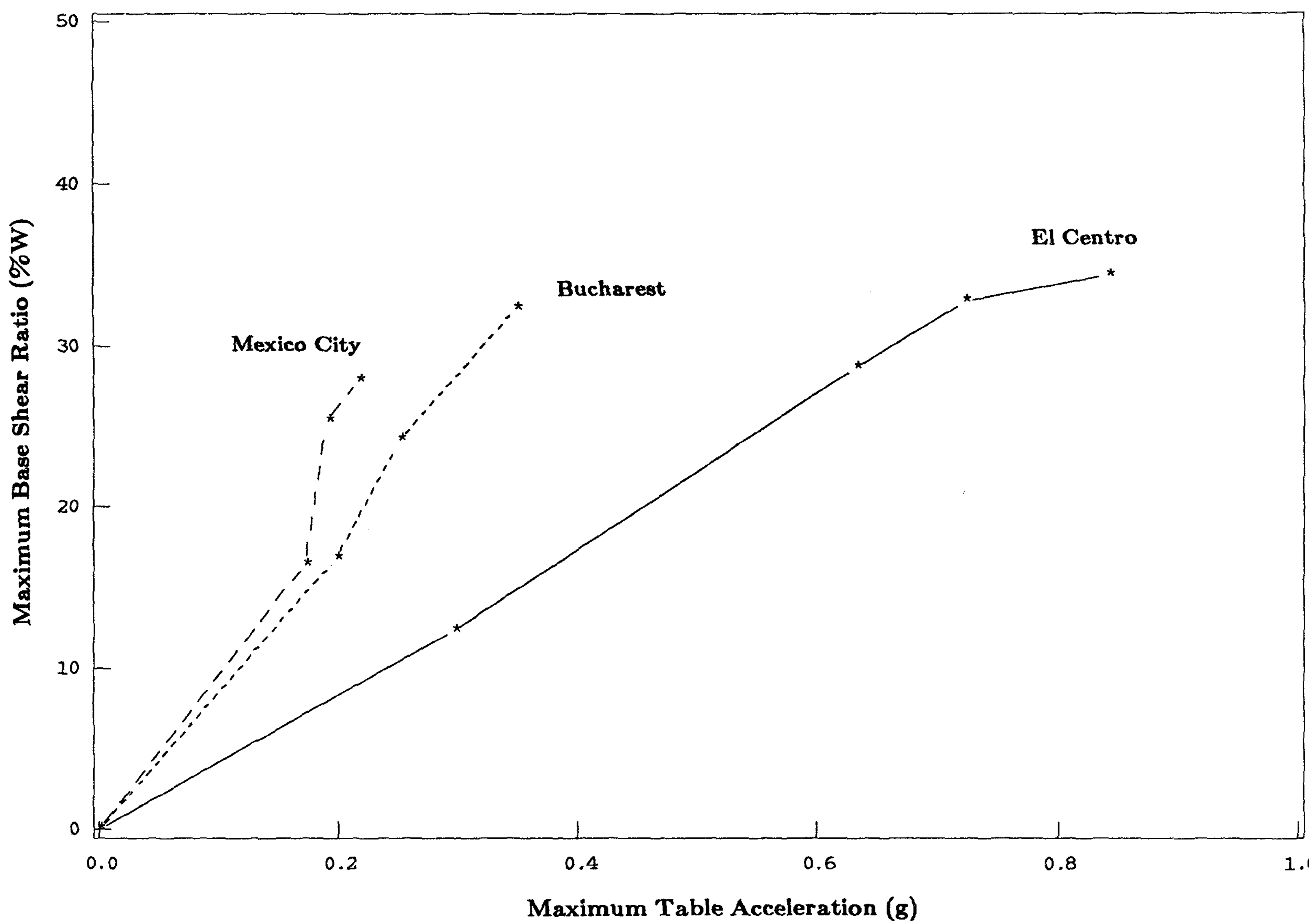

FIGURE 6.6 PEAK BASE SHEAR RATIO VS. PEAK TABLE ACCELERATION FOR FREE-TO-UPLIFT MODEL

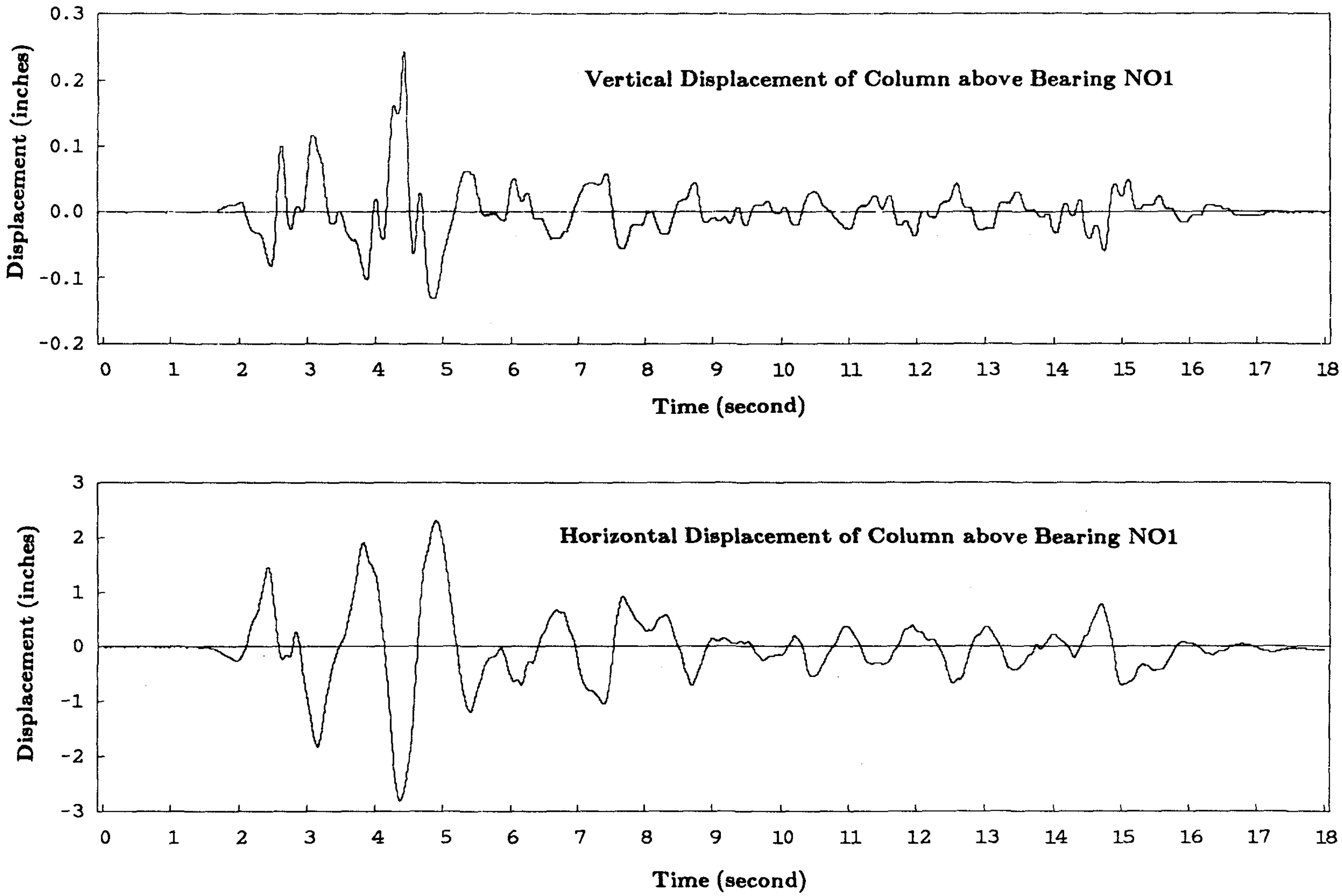

FIGURE 6.7 BEARING HORIZONTAL DISPLACEMENT AND COLUMN VERTICAL DISPLACEMENT DURING EL CENTRO-0.832g TEST (UPLIFT-RESTRAINED CONDITION)

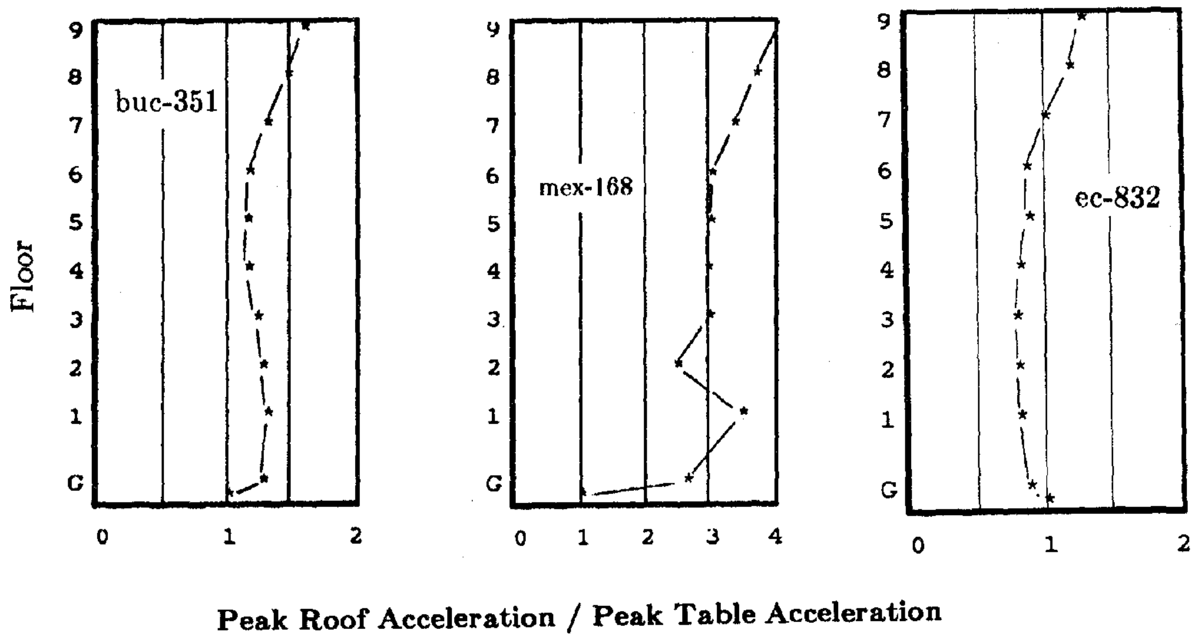

FIGURE 6.8 MAXIMUM STORY ACCELERATION PROFILES FOR THE UPLIFT-RESTRAINED MODEL

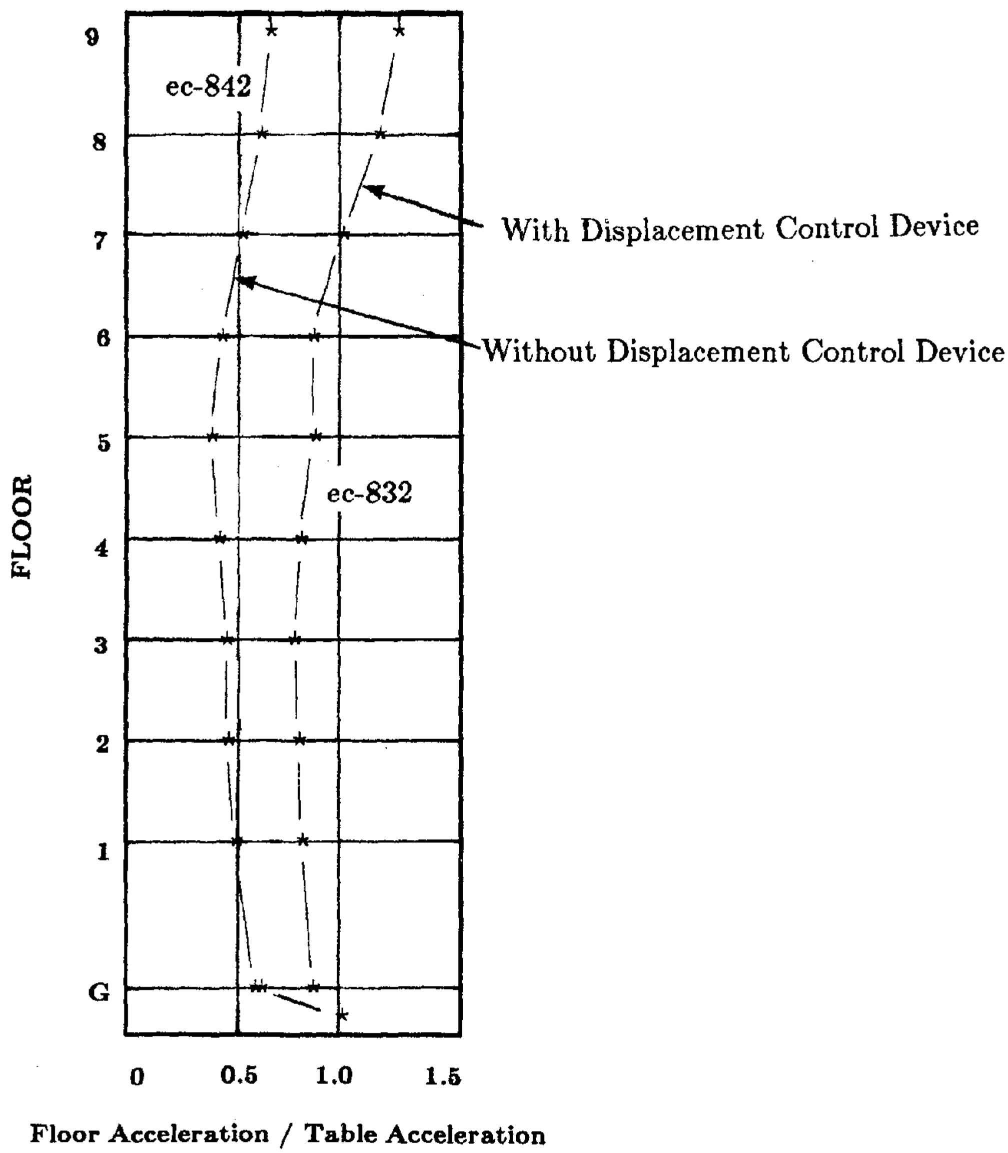

FIGURE 6.9 PROFILES OF PEAK STORY ACCELERATIONS FOR THE FREE-TO-UPLIFT AND UPLIFT-RESTRAINED ISOLATION CONDITIONS

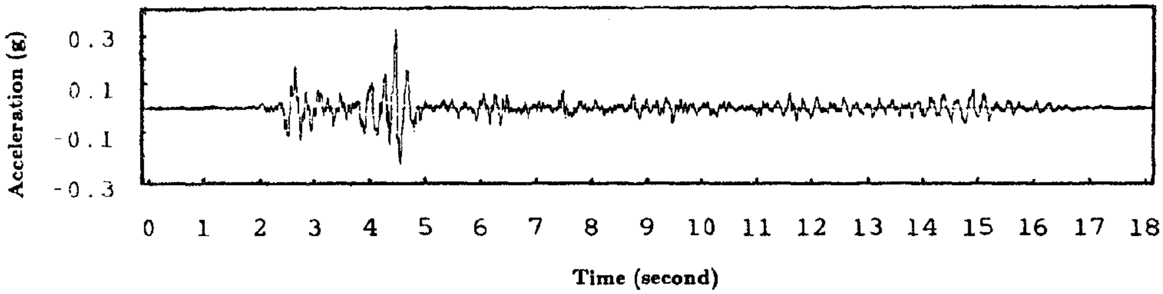

(a) Vertical Acceleration above Bearing NO1

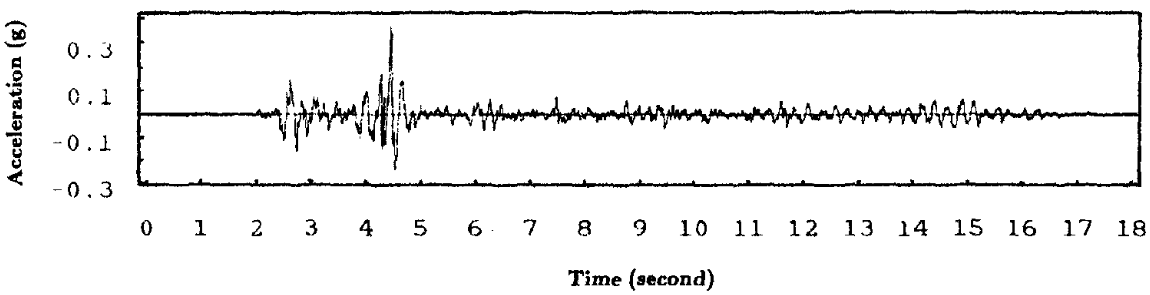

(b) Vertical Acceleration above Bearing NO2

FIGURE 6.10 VERTICAL ACCELERATIONS IN UPLIFT-RESTRAINED MODEL DURING EL CENTRO-0.832g TEST

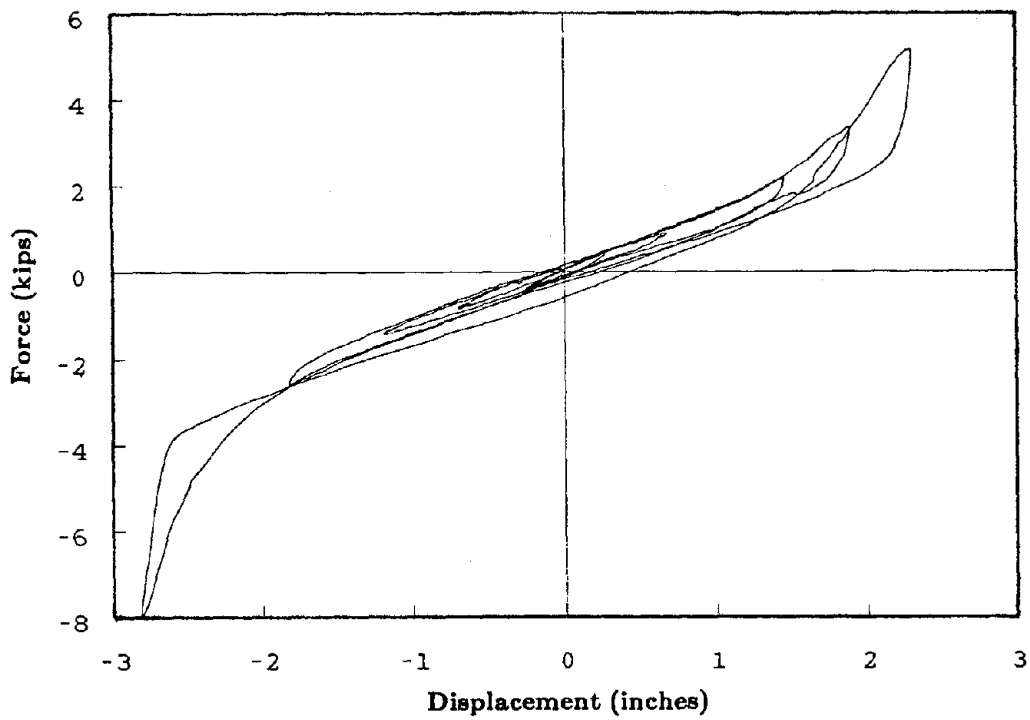

(a) Shear Force vs. Horizontal Displacement

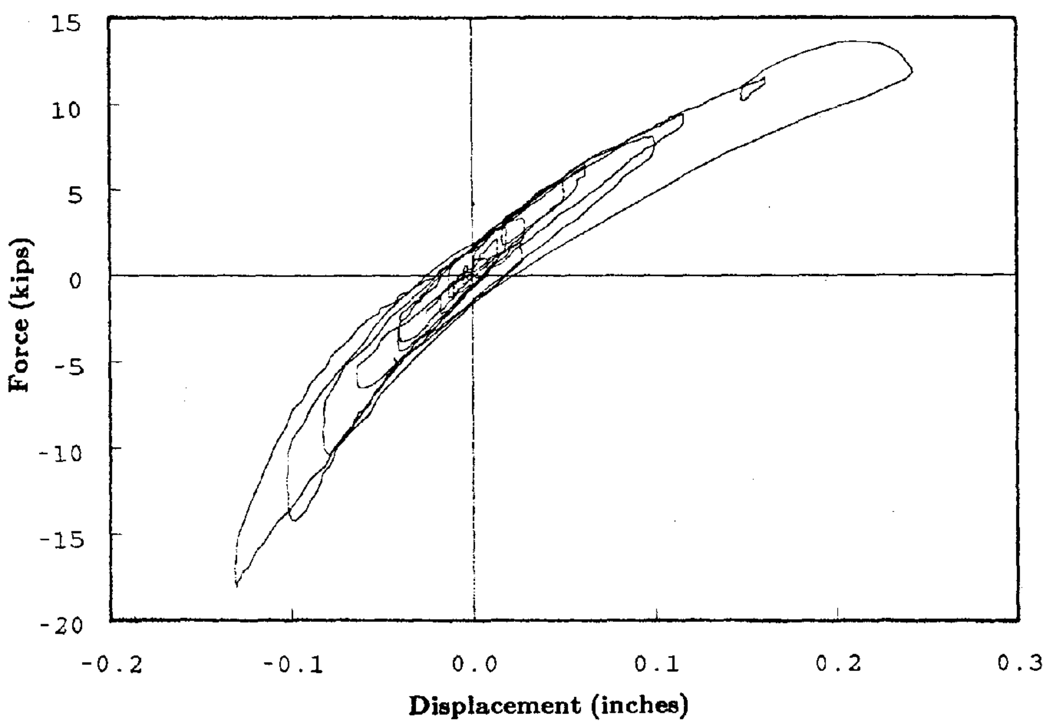

(b) Axial Force vs. Vertical Displacement

FIGURE 6.11 SHEAR AND AXIAL FORCE BEHAVIOR OF BEARINGS IN UPLIFT-RESTRAINED CONDITION DURING EL CENTRO-0.832g TEST

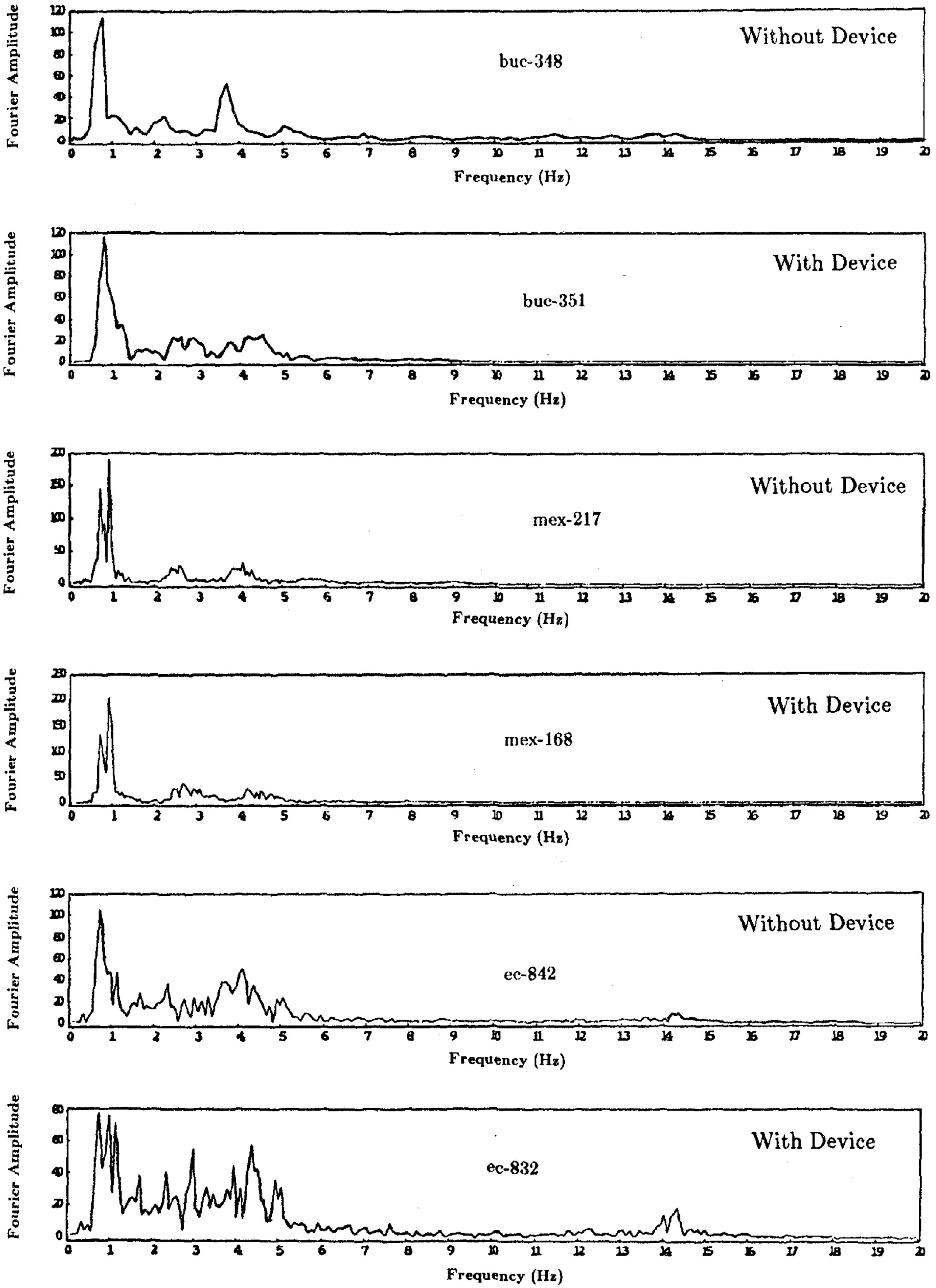

FIGURE 6.12 FFTS OF ROOF ACCELERATION TIME HISTORIES FOR FREE-TO-UPLIFT AND UPLIFT-RESTRAINED MODELS

EARTHQUAKE ENGINEERING RESEARCH CENTER REPORT SERIES

EERC reports are available from the National Information Service for Earthquake Engineering(NISEE) and from the National Technical Information Service(NTIS). Numbers in parentheses are Accession Numbers assigned by the National Technical Information Service; these are followed by a price code. Contact NTIS, 5285 Port Royal Road, Springfield Virginia, 22161 for more information. Reports without Accession Numbers were not available from NTIS at the time of printing. For a current complete list of EERC reports (from EERC 67-1) and availablity information, please contact University of California, EERC, NISEE, 1301 South 46th Street, Richmond, California 94804.

UCB/EERC-80/01 "Earthquake Response of Concrete Gravity Dams Including Hydrodynamic and Foundation Interaction Effects," by Chopra, A.K., Chakrabarti, P. and Gupta, S., January 1980, (AD-A087297)A10.

UCB/EERC-80/02 "Rocking Response of Rigid Blocks to Earthquakes," by Yim, C.S., Chopra, A.K. and Penzien, J., January 1980, (PB80 166 002)A04.

UCB/EERC-80/03 "Optimum Inelastic Design of Seismic-Resistant Reinforced Concrete Frame Structures," by Zagajeski, S.W. and Bertero, V.V., January 1980, (PB80 164 635)A06.

UCB/EERC-80/04 "Effects of Amount and Arrangement of Wall-Panel Reinforcement on Hysteretic Behavior of Reinforced Concrete Walls," by Iliya, R. and Bertero, V.V., February 1980, (PB81 122 525)A09.

UCB/EERC-80/05 "Shaking Table Research on Concrete Dam Models," by Niwa, A. and Clough, R.W., September 1980, (PB81 122 368)A06.

UCB/EERC-80/06 "The Design of Steel Energy-Absorbing Restrainers and their Incorporation into Nuclear Power Plants for Enhanced Safety (Vol 1a): Piping with Energy Absorbing Restrainers: Parameter Study on Small Systems," by Powell, G.H., Oughourlian, C. and Simons, J., June 1980.

UCB/EERC-80/07 "Inelastic Torsional Response of Structures Subjected to Earthquake Ground Motions," by Yamazaki, Y., April 1980, (PB81 122 327)A08.

UCB/EERC-80/08 "Study of X-Braced Steel Frame Structures under Earthquake Simulation," by Ghanaat, Y., April 1980, (PB81 122 335)A11.

UCB/EERC-80/09 "Hybrid Modelling of Soil-Structure Interaction," by Gupta, S., Lin, T.W. and Penzien, J., May 1980, (PB81 122 319)A07.

UCB/EERC-80/10 "General Applicability of a Nonlinear Model of a One Story Steel Frame," by Sveinsson, B.I. and McNiven, H.D., May 1980, (PB81 124 877)A06.

UCB/EERC-80/11 "A Green-Function Method for Wave Interaction with a Submerged Body," by Kioka, W., April 1980, (PB81 122 269)A07.

UCB/EERC-80/12 "Hydrodynamic Pressure and Added Mass for Axisymmetric Bodies.," by Nilrat, F., May 1980, (PB81 122 343)A08.

UCB/EERC-80/13 "Treatment of Non-Linear Drag Forces Acting on Offshore Platforms," by Dao, B.V. and Penzien, J., May 1980, (PB81 153 413)A07.

UCB/EERC-80/14 "2D Plane/Axisymmetric Solid Element (Type 3-Elastic or Elastic-Perfectly Plastic) for the ANSR-II Program," by Mondkar, D.P. and Powell, G.H., July 1980, (PB81 122 350)A03.

UCB/EERC-80/15 "A Response Spectrum Method for Random Vibrations," by Der Kiureghian, A., June 1981, (PB81 122 301)A03.

UCB/EERC-80/16 "Cyclic Inelastic Buckling of Tubular Steel Braces," by Zayas, V.A., Popov, E.P. and Martin, S.A., June 1981, (PB81 124 885)A10.

UCB/EERC-80/17 "Dynamic Response of Simple Arch Dams Including Hydrodynamic Interaction," by Porter, C.S. and Chopra, A.K., July 1981, (PB81 124 000)A13.

UCB/EERC-80/18 "Experimental Testing of a Friction Damped Aseismic Base Isolation System with Fail-Safe Characteristics," by Kelly, J.M., Beucke, K.E. and Skinner, M.S., July 1980, (PB81 148 595)A04.

UCB/EERC-80/19 "The Design of Steel Emergy-Absorbing Restrainers and their Incorporation into Nuclear Power Plants for Enhanced Safety (Vol.1B): Stochastic Seismic Analyses of Nuclear Power Plant Structures and Piping Systems Subjected to Multiple Supported Excitations," by Lee, M.C. and Penzien, J., June 1980, (PB82 201 872)A08.

UCB/EERC-80/20 "The Design of Steel Energy-Absorbing Restrainers and their Incorporation into Nuclear Power Plants for Enhanced Safety (Vol 1C): Numerical Method for Dynamic Substructure Analysis," by Dickens, J.M. and Wilson, E.L., June 1980.

UCB/EERC-80/21 "The Design of Steel Energy-Absorbing Restrainers and their Incorporation into Nuclear Power Plants for Enhanced Safety (Vol 2): Development and Testing of Restraints for Nuclear Piping Systems," by Kelly, J.M. and Skinner, M.S., June 1980.

UCB/EERC-80/22 "3D Solid Element (Type 4-Elastic or Elastic-Perfectly-Plastic) for the ANSR-II Program," by Mondkar, D.P. and Powell, G.H., July 1980, (PB81 123 242)A03.

UCB/EERC-80/23 "Gap-Friction Element (Type 5) for the Ansr-II Program," by Mondkar, D.P. and Powell, G.H., July 1980, (PB81 122 285)A03.

UCB/EERC-80/24 "U-Bar Restraint Element (Type 11) for the ANSR-II Program," by Oughourlian, C. and Powell, G.H., July 1980, (PB81 122 293)A03.

UCB/EERC-80/25 "Testing of a Natural Rubber Base Isolation System by an Explosively Simulated Earthquake," by Kelly, J.M., August 1980, (PB81 201 360)A04.

UCB/EERC-80/26 "Input Identification from Structural Vibrational Response," by Hu, Y., August 1980, (PB81 152 308)A05.

UCB/EERC-80/27 "Cyclic Inelastic Behavior of Steel Offshore Structures," by Zayas, V.A., Mahin, S.A. and Popov, E.P., August 1980, (PB81 196 180)A15.

UCB/EERC-80/28 "Shaking Table Testing of a Reinforced Concrete Frame with Biaxial Response," by Oliva, M.G., October 1980, (PB81 154 304)A10.

UCB/EERC-80/29 "Dynamic Properties of a Twelve-Story Prefabricated Panel Building," by Bouwkamp, J.G., Kollegger, J.P. and Stephen, R.M., October 1980, (PB82 138 777)A07.

UCB/EERC-80/30 "Dynamic Properties of an Eight-Story Prefabricated Panel Building," by Bouwkamp, J.G., Kollegger, J.P. and Stephen, R.M., October 1980, (PB81 200 313)A05.

UCB/EERC-80/31 "Predictive Dynamic Response of Panel Type Structures under Earthquakes," by Kollegger, J.P. and Bouwkamp, J.G., October 1980, (PB81 152 316)A04.

UCB/EERC-80/32 "The Design of Steel Energy-Absorbing Restrainers and their Incorporation into Nuclear Power Plants for Enhanced Safety (Vol 3): Testing of Commercial Steels in Low-Cycle Torsional Fatique," by Spanner, P., Parker, E.R., Jongewaard, E. and Dory, M., 1980.

UCB/EERC-80/33 "The Design of Steel Energy-Absorbing Restrainers and their Incorporation into Nuclear Power Plants for Enhanced Safety (Vol 4): Shaking Table Tests of Piping Systems with Energy-Absorbing Restrainers," by Stiemer, S.F. and Godden, W.G., September 1980, (PB82 201 880)A05.

UCB/EERC-80/34 "The Design of Steel Energy-Absorbing Restrainers and their Incorporation into Nuclear Power Plants for Enhanced Safety (Vol 5): Summary Report," by Spencer, P., 1980.

UCB/EERC-80/35 "Experimental Testing of an Energy-Absorbing Base Isolation System," by Kelly, J.M., Skinner, M.S. and Beucke, K.E., October 1980, (PB81 154 072)A04.

UCB/EERC-80/36 "Simulating and Analyzing Artificial Non-Stationary Earth Ground Motions," by Nau, R.F., Oliver, R.M. and Pister, K.S., October 1980, (PB81 153 397)A04.

UCB/EERC-80/37 "Earthquake Engineering at Berkeley - 1980," by , September 1980, (PB81 205 674)A09.

UCB/EERC-80/38 "Inelastic Seismic Analysis of Large Panel Buildings," by Schricker, V. and Powell, G.H., September 1980, (PB81 154 338)A13.

UCB/EERC-80/39 "Dynamic Response of Embankment, Concrete-Gavity and Arch Dams Including Hydrodynamic Interation," by Hall, J.F. and Chopra, A.K., October 1980, (PB81 152 324)A11.

UCB/EERC-80/40 "Inelastic Buckling of Steel Struts under Cyclic Load Reversal.," by Black, R.G. , Wenger, W.A. and Popov, E.P., October 1980, (PB81 154 312)A08.

UCB/EERC-80/41 "Influence of Site Characteristics on Buildings Damage during the October 3,1974 Lima Earthquake," by Repetto, P., Arango, I. and Seed, H.B., September 1980, (PB81 161 739)A05.

UCB/EERC-80/42 "Evaluation of a Shaking Table Test Program on Response Behavior of a Two Story Reinforced Concrete Frame," by Blondet, J.M., Clough, R.W. and Mahin, S.A., December 1980, (PB82 196 544)A11.

UCB/EERC-80/43 "Modelling of Soil-Structure Interaction by Finite and Infinite Elements," by Medina, F., December 1980, (PB81 229 270)A04.

UCB/EERC-81/01 "Control of Seismic Response of Piping Systems and Other Structures by Base Isolation," by Kelly, J.M., January 1981, (PB81 200 735)A05.

UCB/EERC-81/02 "OPTNSR- An Interactive Software System for Optimal Design of Statically and Dynamically Loaded Structures with Nonlinear Response," by Bhatti, M.A., Ciampi, V. and Pister, K.S., January

1981, (PB81 218 851)A09.

UCB/EERC-81/03 "Analysis of Local Variations in Free Field Seismic Ground Motions," by Chen, J.-C., Lysmer, J. and Seed, H.B., January 1981, (AD-A099508)A13.

UCB/EERC-81/04 "Inelastic Structural Modeling of Braced Offshore Platforms for Seismic Loading. ," by Zayas, V.A., Shing, P.-S.B., Mahin, S.A. and Popov, E.P., January 1981, (PB82 138 777)A07.

UCB/EERC-81/05 "Dynamic Response of Light Equipment in Structures," by Der Kiureghian, A., Sackman, J.L. and Nour-Omid, B., April 1981, (PB81 218 497)A04.

UCB/EERC-81/06 "Preliminary Experimental Investigation of a Broad Base Liquid Storage Tank," by Bouwkamp, J.G., Kollegger, J.P. and Stephen, R.M., May 1981, (PB82 140 385)A03.

UCB/EERC-81/07 "The Seismic Resistant Design of Reinforced Concrete Coupled Structural Walls," by Aktan, A.E. and Bertero, V.V., June 1981, (PB82 113 358)A11.

UCB/EERC-81/08 "Unassigned," by Unassigned, 1981.

UCB/EERC-81/09 "Experimental Behavior of a Spatial Piping System with Steel Energy Absorbers Subjected to a Simulated Differential Seismic Input," by Stiemer, S.F., Godden, W.G. and Kelly, J.M., July 1981, (PB82 201 898)A04.

UCB/EERC-81/10 "Evaluation of Seismic Design Provisions for Masonry in the United States," by Sveinsson, B.I., Mayes, R.L. and McNiven, H.D., August 1981, (PB82 166 075)A08.

UCB/EERC-81/11 "Two-Dimensional Hybrid Modelling of Soil-Structure Interaction," by Tzong, T.-J., Gupta, S. and Penzien, J., August 1981, (PB82 142 118)A04.

UCB/EERC-81/12 "Studies on Effects of Infills in Seismic Resistant R/C Construction," by Brokken, S. and Bertero, V.V., October 1981, (PB82 166 190)A09.

UCB/EERC-81/13 "Linear Models to Predict the Nonlinear Seismic Behavior of a One-Story Steel Frame," by Valdimarsson, H., Shah, A.H. and McNiven, H.D., September 1981, (PB82 138 793)A07.

UCB/EERC-81/14 "TLUSH: A Computer Program for the Three-Dimensional Dynamic Analysis of Earth Dams," by Kagawa, T., Mejia, L.H., Seed, H.B. and Lysmer, J., September 1981, (PB82 139 940)A06.

UCB/EERC-81/15 "Three Dimensional Dynamic Response Analysis of Earth Dams," by Mejia, L.H. and Seed, H.B., September 1981, (PB82 137 274)A12.

UCB/EERC-81/16 "Experimental Study of Lead and Elastomeric Dampers for Base Isolation Systems," by Kelly, J.M. and Hodder, S.B., October 1981, (PB82 166 182)A05.

UCB/EERC-81/17 "The Influence of Base Isolation on the Seismic Response of Light Secondary Equipment," by Kelly, J.M., April 1981, (PB82 255 266)A04.

UCB/EERC-81/18 "Studies on Evaluation of Shaking Table Response Analysis Procedures," by Blondet, J. Marcial, November 1981, (PB82 197 278)A10.

UCB/EERC-81/19 "DELIGHT.STRUCT: A Computer-Aided Design Environment for Structural Engineering. ," by Balling, R.J., Pister, K.S. and Polak, E., December 1981, (PB82 218 496)A07.

UCB/EERC-81/20 "Optimal Design of Seismic-Resistant Planar Steel Frames," by Balling, R.J., Ciampi, V. and Pister, K.S., December 1981, (PB82 220 179)A07.

UCB/EERC-82/01 "Dynamic Behavior of Ground for Seismic Analysis of Lifeline Systems," by Sato, T. and Der Kiureghian, A., January 1982, (PB82 218 926)A05.

UCB/EERC-82/02 "Shaking Table Tests of a Tubular Steel Frame Model," by Ghanaat, Y. and Clough, R.W., January 1982, (PB82 220 161)A07.

UCB/EERC-82/03 "Behavior of a Piping System under Seismic Excitation: Experimental Investigations of a Spatial Piping System supported by Mechanical Shock Arrestors," by Schneider, S., Lee, H.-M. and Godden, W. G., May 1982, (PB83 172 544)A09.

UCB/EERC-82/04 "New Approaches for the Dynamic Analysis of Large Structural Systems," by Wilson, E.L., June 1982, (PB83 148 080)A05.

UCB/EERC-82/05 "Model Study of Effects of Damage on the Vibration Properties of Steel Offshore Platforms," by Shahrivar, F. and Bouwkamp, J.G., June 1982, (PB83 148 742)A10.

UCB/EERC-82/06 "States of the Art and Pratice in the Optimum Seismic Design and Analytical Response Prediction of R/C Frame Wall Structures," by Aktan, A.E. and Bertero, V.V., July 1982, (PB83 147 736)A05.

UCB/EERC-82/07 "Further Study of the Earthquake Response of a Broad Cylindrical Liquid-Storage Tank Model," by Manos, G.C. and Clough, R.W., July 1982, (PB83 147 744)A11.

UCB/EERC-82/08 "An Evaluation of the Design and Analytical Seismic Response of a Seven Story Reinforced Concrete Frame," by Charney, F.A. and Bertero, V.V., July 1982, (PB83 157 628)A09.

UCB/EERC-82/09 "Fluid-Structure Interactions: Added Mass Computations for Incompressible Fluid. ," by Kuo, J.S.-H., August 1982, (PB83 156 281)A07.

UCB/EERC-82/10 "Joint-Opening Nonlinear Mechanism: Interface Smeared Crack Model," by Kuo, J.S.-H., August 1982, (PB83 149 195)A05.

UCB/EERC-82/11 "Dynamic Response Analysis of Techi Dam," by Clough, R.W., Stephen, R.M. and Kuo, J.S.-H., August 1982, (PB83 147 496)A06.

UCB/EERC-82/12 "Prediction of the Seismic Response of R/C Frame-Coupled Wall Structures," by Aktan, A.E., Bertero, V.V. and Piazzo, M., August 1982, (PB83 149 203)A09.

UCB/EERC-82/13 "Preliminary Report on the Smart 1 Strong Motion Array in Taiwan," by Bolt, B.A. , Loh, C.H., Penzien, J. and Tsai, Y.B., August 1982, (PB83 159 400)A10.

UCB/EERC-82/14 "Shaking-Table Studies of an Eccentrically X-Braced Steel Structure," by Yang, M.S., September 1982, (PB83 260 778)A12.

UCB/EERC-82/15 "The Performance of Stairways in Earthquakes," by Roha, C., Axley, J.W. and Bertero, V.V., September 1982, (PB83 157 693)A07.

UCB/EERC-82/16 "The Behavior of Submerged Multiple Bodies in Earthquakes," by Liao, W.-G., September 1982, (PB83 158 709)A07.

UCB/EERC-82/17 "Effects of Concrete Types and Loading Conditions on Local Bond-Slip Relationships," by Cowell, A.D., Popov, E.P. and Bertero, V.V., September 1982, (PB83 153 577)A04.

UCB/EERC-82/18 "Mechanical Behavior of Shear Wall Vertical Boundary Members: An Experimental Investigation," by Wagner, M.T. and Bertero, V.V., October 1982, (PB83 159 764)A05.

UCB/EERC-82/19 "Experimental Studies of Multi-support Seismic Loading on Piping Systems," by Kelly, J.M. and Cowell, A.D., November 1982.

UCB/EERC-82/20 "Generalized Plastic Hinge Concepts for 3D Beam-Column Elements," by Chen, P. F.-S. and Powell, G.H., November 1982, (PB83 247 981)A13.

UCB/EERC-82/21 "ANSR-II: General Computer Program for Nonlinear Structural Analysis," by Oughourlian, C.V. and Powell, G.H., November 1982, (PB83 251 330)A12.

UCB/EERC-82/22 "Solution Strategies for Statically Loaded Nonlinear Structures," by Simons, J.W. and Powell, G.H., November 1982, (PB83 197 970)A06.

UCB/EERC-82/23 "Analytical Model of Deformed Bar Anchorages under Generalized Excitations," by Ciampi, V., Eligehausen, R., Bertero, V.V. and Popov, E.P., November 1982, (PB83 169 532)A06.

UCB/EERC-82/24 "A Mathematical Model for the Response of Masonry Walls to Dynamic Excitations," by Sucuoglu, H., Mengi, Y. and McNiven, H.D., November 1982, (PB83 169 011)A07.

UCB/EERC-82/25 "Earthquake Response Considerations of Broad Liquid Storage Tanks," by Cambra, F.J., November 1982, (PB83 251 215)A09.

UCB/EERC-82/26 "Computational Models for Cyclic Plasticity, Rate Dependence and Creep," by Mosaddad, B. and Powell, G.H., November 1982, (PB83 245 829)A08.

UCB/EERC-82/27 "Inelastic Analysis of Piping and Tubular Structures," by Mahasuverachai, M. and Powell, G.H., November 1982, (PB83 249 987)A07.

UCB/EERC-83/01 "The Economic Feasibility of Seismic Rehabilitation of Buildings by Base Isolation," by Kelly, J.M., January 1983, (PB83 197 988)A05.

UCB/EERC-83/02 "Seismic Moment Connections for Moment-Resisting Steel Frames.," by Popov, E.P., January 1983, (PB83 195 412)A04.

UCB/EERC-83/03 "Design of Links and Beam-to-Column Connections for Eccentrically Braced Steel Frames," by Popov, E.P. and Malley, J.O., January 1983, (PB83 194 811)A04.

UCB/EERC-83/04 "Numerical Techniques for the Evaluation of Soil-Structure Interaction Effects in the Time Domain," by Bayo, E. and Wilson, E.L., February 1983, (PB83 245 605)A09.

UCB/EERC-83/05 "A Transducer for Measuring the Internal Forces in the Columns of a Frame-Wall Reinforced Concrete Structure," by Sause, R. and Bertero, V.V., May 1983, (PB84 119 494)A06.

UCB/EERC-83/06 "Dynamic Interactions Between Floating Ice and Offshore Structures," by Croteau, P., May 1983, (PB84 119 486)A16.

UCB/EERC-83/07 "Dynamic Analysis of Multiply Tuned and Arbitrarily Supported Secondary Systems. ," by Igusa, T. and Der Kiureghian, A., July 1983, (PB84 118 272)A11.

UCB/EERC-83/08 "A Laboratory Study of Submerged Multi-body Systems in Earthquakes," by Ansari, G.R., June 1983, (PB83 261 842)A17.

UCB/EERC-83/09 "Effects of Transient Foundation Uplift on Earthquake Response of Structures," by Yim, C.-S. and Chopra, A.K., June 1983, (PB83 261 396)A07.

UCB/EERC-83/10 "Optimal Design of Friction-Braced Frames under Seismic Loading," by Austin, M.A. and Pister, K.S., June 1983, (PB84 119 288)A06.

UCB/EERC-83/11 "Shaking Table Study of Single-Story Masonry Houses: Dynamic Performance under Three Component Seismic Input and Recommendations," by Manos, G.C., Clough, R.W. and Mayes, R.L., July 1983, (UCB/EERC-83/11)A08.

UCB/EERC-83/12 "Experimental Error Propagation in Pseudodynamic Testing," by Shiing, P.B. and Mahin, S.A., June 1983, (PB84 119 270)A09.

UCB/EERC-83/13 "Experimental and Analytical Predictions of the Mechanical Characteristics of a 1/5-scale Model of a 7-story R/C Frame-Wall Building Structure," by Aktan, A.E., Bertero, V.V., Chowdhury, A.A. and Nagashima, T., June 1983, (PB84 119 213)A07.

UCB/EERC-83/14 "Shaking Table Tests of Large-Panel Precast Concrete Building System Assemblages," by Oliva, M.G. and Clough, R.W., June 1983, (PB86 110 210/AS)A11.

UCB/EERC-83/15 "Seismic Behavior of Active Beam Links in Eccentrically Braced Frames," by Hjelmstad, K.D. and Popov, E.P., July 1983, (PB84 119 676)A09.

UCB/EERC-83/16 "System Identification of Structures with Joint Rotation," by Dimsdale, J.S., July 1983, (PB84 192 210)A06.

UCB/EERC-83/17 "Construction of Inelastic Response Spectra for Single-Degree-of-Freedom Systems," by Mahin, S. and Lin, J., June 1983, (PB84 208 834)A05.

UCB/EERC-83/18 "Interactive Computer Analysis Methods for Predicting the Inelastic Cyclic Behaviour of Structural Sections," by Kaba, S. and Mahin, S., July 1983, (PB84 192 012)A06.

UCB/EERC-83/19 "Effects of Bond Deterioration on Hysteretic Behavior of Reinforced Concrete Joints," by Filippou, F.C., Popov, E.P. and Bertero, V.V., August 1983, (PB84 192 020)A10.

UCB/EERC-83/20 "Analytical and Experimental Correlation of Large-Panel Precast Building System Performance," by Oliva, M.G., Clough, R.W., Velkov, M. and Gavrilovic, P., November 1983.

UCB/EERC-83/21 "Mechanical Characteristics of Materials Used in a 1/5 Scale Model of a 7-Story Reinforced Concrete Test Structure," by Bertero, V.V., Aktan, A.E., Harris, H.G. and Chowdhury, A.A., October 1983, (PB84 193 697)A05.

UCB/EERC-83/22 "Hybrid Modelling of Soil-Structure Interaction in Layered Media," by Tzong, T.-J. and Penzien, J., October 1983, (PB84 192 178)A08.

UCB/EERC-83/23 "Local Bond Stress-Slip Relationships of Deformed Bars under Generalized Excitations," by Eligehausen, R., Popov, E.P. and Bertero, V.V., October 1983, (PB84 192 848)A09.

UCB/EERC-83/24 "Design Considerations for Shear Links in Eccentrically Braced Frames," by Malley, J.O. and Popov, E.P., November 1983, (PB84 192 186)A07.

UCB/EERC-84/01 "Pseudodynamic Test Method for Seismic Performance Evaluation: Theory and Implementation," by Shing, P.-S. B. and Mahin, S.A., January 1984, (PB84 190 644)A08.

UCB/EERC-84/02 "Dynamic Response Behavior of Kiang Hong Dian Dam," by Clough, R.W., Chang, K.-T., Chen, H.-Q. and Stephen, R.M., April 1984, (PB84 209 402)A08.

UCB/EERC-84/03 "Refined Modelling of Reinforced Concrete Columns for Seismic Analysis," by Kaba, S.A. and Mahin, S.A., April 1984, (PB84 234 384)A06.

UCB/EERC-84/04 "A New Floor Response Spectrum Method for Seismic Analysis of Multiply Supported Secondary Systems," by Asfura, A. and Der Kiureghian, A., June 1984, (PB84 239 417)A06.

UCB/EERC-84/05 "Earthquake Simulation Tests and Associated Studies of a 1/5th-scale Model of a 7-Story R/C Frame-Wall Test Structure," by Bertero, V.V., Aktan, A.E., Charney, F.A. and Sause, R., June 1984, (PB84 239 409)A09.

UCB/EERC-84/06 "R/C Structural Walls: Seismic Design for Shear," by Aktan, A.E. and Bertero, V.V., 1984.

UCB/EERC-84/07 "Behavior of Interior and Exterior Flat-Plate Connections subjected to Inelastic Load Reversals," by Zee, H.L. and Moehle, J.P., August 1984, (PB86 117 629/AS)A07.

UCB/EERC-84/08 "Experimental Study of the Seismic Behavior of a Two-Story Flat-Plate Structure. ," by Moehle, J.P. and Diebold, J.W., August 1984, (PB86 122 553/AS)A12.

UCB/EERC-84/09 "Phenomenological Modeling of Steel Braces under Cyclic Loading," by Ikeda, K., Mahin, S.A. and Dermitzakis, S.N., May 1984, (PB86 132 198/AS)A08.

UCB/EERC-84/10 "Earthquake Analysis and Response of Concrete Gravity Dams," by Fenves, G. and Chopra, A.K., August 1984, (PB85 193 902/AS)A11.

UCB/EERC-84/11 "EAGD-84: A Computer Program for Earthquake Analysis of Concrete Gravity Dams," by Fenves, G. and Chopra, A.K., August 1984, (PB85 193 613/AS)A05.

UCB/EERC-84/12 "A Refined Physical Theory Model for Predicting the Seismic Behavior of Braced Steel Frames," by Ikeda, K. and Mahin, S.A., July 1984, (PB85 191 450/AS)A09.

UCB/EERC-84/13 "Earthquake Engineering Research at Berkeley - 1984," by , August 1984, (PB85 197 341/AS)A10.

UCB/EERC-84/14 "Moduli and Damping Factors for Dynamic Analyses of Cohesionless Soils," by Seed, H.B., Wong, R.T., Idriss, I.M. and Tokimatsu, K., September 1984, (PB85 191 468/AS)A04.

UCB/EERC-84/15 "The Influence of SPT Procedures in Soil Liquefaction Resistance Evaluations," by Seed, H.B., Tokimatsu, K., Harder, L.F. and Chung, R.M., October 1984, (PB85 191 732/AS)A04.

UCB/EERC-84/16 "Simplified Procedures for the Evaluation of Settlements in Sands Due to Earthquake Shaking," by Tokimatsu, K. and Seed, H.B., October 1984, (PB85 197 887/AS)A03.

UCB/EERC-84/17 "Evaluation of Energy Absorption Characteristics of Bridges under Seismic Conditions," by Imbsen, R.A. and Penzien, J., November 1984.

UCB/EERC-84/18 "Structure-Foundation Interactions under Dynamic Loads," by Liu, W.D. and Penzien, J., November 1984, (PB87 124 889/AS)A11.

UCB/EERC-84/19 "Seismic Modelling of Deep Foundations," by Chen, C.-H. and Penzien, J., November 1984, (PB87 124 798/AS)A07.

UCB/EERC-84/20 "Dynamic Response Behavior of Quan Shui Dam," by Clough, R.W., Chang, K.-T., Chen, H.-Q., Stephen, R.M., Ghanaat, Y. and Qi, J.-H., November 1984, (PB86 115177/AS)A07.

UCB/EERC-85/01 "Simplified Methods of Analysis for Earthquake Resistant Design of Buildings," by Cruz, E.F. and Chopra, A.K., February 1985, (PB86 112299/AS)A12.

UCB/EERC-85/02 "Estimation of Seismic Wave Coherency and Rupture Velocity using the SMART 1 Strong-Motion Array Recordings," by Abrahamson, N.A., March 1985, (PB86 214 343)A07.

UCB/EERC-85/03 "Dynamic Properties of a Thirty Story Condominium Tower Building," by Stephen, R.M., Wilson, E.L. and Stander, N., April 1985, (PB86 118965/AS)A06.

UCB/EERC-85/04 "Development of Substructuring Techniques for On-Line Computer Controlled Seismic Performance Testing," by Dermitzakis, S. and Mahin, S., February 1985, (PB86 132941/AS)A08.

UCB/EERC-85/05 "A Simple Model for Reinforcing Bar Anchorages under Cyclic Excitations," by Filippou, F.C., March 1985, (PB86 112 919/AS)A05.

UCB/EERC-85/06 "Racking Behavior of Wood-framed Gypsum Panels under Dynamic Load," by Oliva, M.G., June 1985.

UCB/EERC-85/07 "Earthquake Analysis and Response of Concrete Arch Dams," by Fok, K.-L. and Chopra, A.K., June 1985, (PB86 139672/AS)A10.

UCB/EERC-85/08 "Effect of Inelastic Behavior on the Analysis and Design of Earthquake Resistant Structures," by Lin, J.P. and Mahin, S.A., June 1985, (PB86 135340/AS)A08.

UCB/EERC-85/09 "Earthquake Simulator Testing of a Base-Isolated Bridge Deck," by Kelly, J.M., Buckle, I.G. and Tsai, H.-C., January 1986, (PB87 124 152/AS)A06.

UCB/EERC-85/10 "Simplified Analysis for Earthquake Resistant Design of Concrete Gravity Dams," by Fenves, G. and Chopra, A.K., June 1986, (PB87 124 160/AS)A08.

UCB/EERC-85/11 "Dynamic Interaction Effects in Arch Dams," by Clough, R.W., Chang, K.-T., Chen, H.-Q. and Ghanaat, Y., October 1985, (PB86 135027/AS)A05.

UCB/EERC-85/12 "Dynamic Response of Long Valley Dam in the Mammoth Lake Earthquake Series of May 25-27, 1980," by Lai, S. and Seed, H.B., November 1985, (PB86 142304/AS)A05.

UCB/EERC-85/13 "A Methodology for Computer-Aided Design of Earthquake-Resistant Steel Structures," by Austin, M.A., Pister, K.S. and Mahin, S.A., December 1985, (PB86 159480/AS)A10 .

UCB/EERC-85/14 "Response of Tension-Leg Platforms to Vertical Seismic Excitations," by Liou, G.-S., Penzien, J. and Yeung, R.W., December 1985, (PB87 124 871/AS)A08.

UCB/EERC-85/15 "Cyclic Loading Tests of Masonry Single Piers: Volume 4 - Additional Tests with Height to Width Ratio of 1," by Sveinsson, B., McNiven, H.D. and Sucuoglu, H., December 1985, (PB87 165 031/AS)A08.

UCB/EERC-85/16 "An Experimental Program for Studying the Dynamic Response of a Steel Frame with a Variety of Infill Partitions," by Yanev, B. and McNiven, H.D., December 1985.

UCB/EERC-86/01 "A Study of Seismically Resistant Eccentrically Braced Steel Frame Systems," by Kasai, K. and Popov, E.P., January 1986, (PB87 124 178/AS)A14.

UCB/EERC-86/02 "Design Problems in Soil Liquefaction," by Seed, H.B., February 1986, (PB87 124 186/AS)A03.

UCB/EERC-86/03 "Implications of Recent Earthquakes and Research on Earthquake-Resistant Design and Construction of Buildings," by Bertero, V.V., March 1986, (PB87 124 194/AS)A05.

UCB/EERC-86/04 "The Use of Load Dependent Vectors for Dynamic and Earthquake Analyses," by Leger, P., Wilson, E.L. and Clough, R.W., March 1986, (PB87 124 202/AS)A12.

UCB/EERC-86/05 "Two Beam-To-Column Web Connections," by Tsai, K.-C. and Popov, E.P., April 1986 , (PB87 124 301/AS)A04.

UCB/EERC-86/06 "Determination of Penetration Resistance for Coarse-Grained Soils using the Becker Hammer Drill," by Harder, L.F. and Seed, H.B., May 1986, (PB87 124 210/AS)A07.

UCB/EERC-86/07 "A Mathematical Model for Predicting the Nonlinear Response of Unreinforced Masonry Walls to In-Plane Earthquake Excitations," by Mengi, Y. and McNiven, H.D., May 1986, (PB87 124 780/AS)A06.

UCB/EERC-86/08 "The 19 September 1985 Mexico Earthquake: Building Behavior," by Bertero, V.V., July 1986.

UCB/EERC-86/09 "EACD-3D: A Computer Program for Three-Dimensional Earthquake Analysis of Concrete Dams," by Fok, K.-L., Hall, J.F. and Chopra, A.K., July 1986, (PB87 124 228/AS)A08.

UCB/EERC-86/10 "Earthquake Simulation Tests and Associated Studies of a 0.3-Scale Model of a Six-Story Concentrically Braced Steel Structure," by Uang, C.-M. and Bertero, V.V., December 1986, (PB87 163564/AS)A17.

UCB/EERC-86/11 "Mechanical Characteristics of Base Isolation Bearings for a Bridge Deck Model Test," by Kelly, J.M., Buckle, I.G. and Koh, C.-G., 1987.

UCB/EERC-86/12 "Modelling of Dynamic Response of Elastomeric Isolation Bearings," by Koh, C.-G. and Kelly, J.M., 1987.

UCB/EERC-87/01 "The FPS Earthquake Resisting System: Experimental Report," by Zayas, V.A., Low, S.S. and Mahin, S.A., June 1987.

UCB/EERC-87/02 "Earthquake Simulator Tests and Associated Studies of a 0.3-Scale Model of a Six-Story Eccentrically Braced Steel Structure," by Whittaker, A., Uang, C.-M. and Bertero, V.V., July 1987.

UCB/EERC-87/03 "A Displacement Control and Uplift Restraint Device for Base-Isolated Structures," by Kelly, J.M., Griffith, M.C. and Aiken, I.G., April 1987.